

AD-A199 612

DTIC FILE COPY

2

AFWAL-TR-88-1042



LASER COMMUNICATION TEST SYSTEM

G. S. Mecherle, et al  
Hughes Aircraft Company, EDSG  
P. O. Box 902  
El Segundo, CA 90245

June 1988

Final Report for September 1986-September 1987

Approved for public release; distribution unlimited.

DTIC  
ELECTE  
SEP 27 1988  
S H D

AVIONICS LABORATORY  
AIR FORCE WRIGHT AERONAUTICAL LABORATORIES  
AIR FORCE SYSTEMS COMMAND  
WRIGHT-PATTERSON AIR FORCE BASE, OHIO 45433-6543

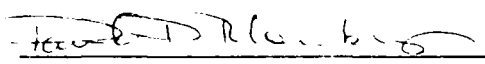
08 8 00 113

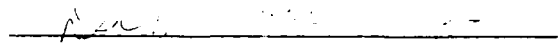
NOTICE

When Government drawings, specifications, or other data are used for any purpose other than in connection with a definitely Government-related procurement, the United States Government incurs no responsibility or any obligation whatsoever. The fact that the Government may have formulated or in any way supplied the said drawings, specifications, or other data, is not to be regarded by implication, or otherwise in any manner construed, as licensing the holder, or any other person or corporation; or as conveying any rights or permission to manufacture, use, or sell any patented invention that may in any way be related thereto.

This report has been reviewed by the Office of Public Affairs (ASD/PA) and is releasable to the National Technical Information Service (NTIS). At NTIS, it will be available to the general public, including foreign nations.

This technical report has been reviewed and is approved for publication.

  
DAVID D. BLOMBERG, 2D LT  
Project Engineer  
Communications Technology Group  
AFWAL Avionics Laboratory

  
DIANE E. SUMMERS, Chief  
Information Transmission Branch  
System Avionics Division

FOR THE COMMANDER

  
CHARLES H. KRUEGER, JR  
Acting Chief  
System Avionics Division  
Avionics Laboratory

If your address has changed, if you wish to be removed from our mailing list, or if the addressee is no longer employed by your organization please notify AFWAL/AAAI, Wright-Patterson AFB, OH 45433-6543 to help us maintain a current mailing list.

Copies of this report should not be returned unless return is required by security considerations, contractual obligations, or notice on a specific document.

Unclassified

SECURITY CLASSIFICATION OF THIS PAGE

REPORT DOCUMENTATION PAGE				
1a. REPORT SECURITY CLASSIFICATION UNCLASSIFIED		1b. RESTRICTIVE MARKINGS		
2a. SECURITY CLASSIFICATION AUTHORITY		3. DISTRIBUTION/AVAILABILITY OF REPORT Approved for public release; distribution is unlimited.		
2b. DECLASSIFICATION/DOWNGRADING SCHEDULE				
4. PERFORMING ORGANIZATION REPORT NUMBER(S)		5. MONITORING ORGANIZATION REPORT NUMBER(S) AFWAL-TR-88-1042		
6a. NAME OF PERFORMING ORGANIZATION Hughes Aircraft Company Electro-Optical Data Sys. Gp.	6b. OFFICE SYMBOL (If applicable)	7a. NAME OF MONITORING ORGANIZATION AFWAL/AAAI		
6c. ADDRESS (City, State and ZIP Code) P. O. Box 902 El Segundo, CA 90245		7b. ADDRESS (City, State and ZIP Code) WPAFB, OH 45433-6543		
8a. NAME OF FUNDING/SPONSORING ORGANIZATION Air Force Avionics Laboratory	8b. OFFICE SYMBOL (If applicable) AFWAL/AAAI	9. PROCUREMENT INSTRUMENT IDENTIFICATION NUMBER F33615-86-C-1073		
8c. ADDRESS (City, State and ZIP Code) Wright Patterson Air Force Base Dayton, OH		10. SOURCE OF FUNDING NOS.		
		PROGRAM ELEMENT NO 63727F	PROJECT NO 2746	TASK NO 04
11. TITLE (Include Security Classification) Laser Communication Test System		WORK UNIT NO 03		
12. PERSONAL AUTHOR(S) Mecherle, G.S.; Rue, A.K.; Pope, G.T.; Benguhe, P.T.; Twete, M.A.				
13a. TYPE OF REPORT Final	13b. TIME COVERED FROM 9/86 TO 9/87	14. DATE OF REPORT (Yr., Mo., Day) 1988 June	15. PAGE COUNT 70	
16. SUPPLEMENTARY NOTATION				
17. COSATI CODES		18. SUBJECT TERMS (Continue on reverse if necessary and identify by block number)		
FIELD	GROUP	SUB. GR.	Laser communication, laser diodes, digital communication, optical communication, video tracking, automatic acquisition.	
19. ABSTRACT (Continue on reverse if necessary and identify by block number)				
<p>A Hughes-developed laser communication terminal was delivered for Air Force Testing that is related to aircraft applications. The terminals employ laser diode transmitters, PIN diode receivers, and provide automatic tracking with a gimbal-mounted video camera and off-gimbal video tracker. The terminals are capable of 20 Kbps full duplex operation over 8-10 miles at sea level. Video tracking offers a legitimate alternative to quadrant tracking.</p> <p>The terminals were modified to provide performance monitors for transmitted signal, received signal, AGC voltage, tracking error, tracker status, and angular position. An automatic acquisition capability with spiral scans was implemented and performed well.</p>				
20. DISTRIBUTION/AVAILABILITY OF ABSTRACT UNCLASSIFIED/UNLIMITED <input checked="" type="checkbox"/> SAME AS RPT <input type="checkbox"/> DTIC USERS <input type="checkbox"/>		21. ABSTRACT SECURITY CLASSIFICATION Unclassified		
22a. NAME OF RESPONSIBLE INDIVIDUAL David D. Blomberg		22b. TELEPHONE NUMBER (Include Area Code) (513) 255-3455	22c. OFFICE SYMBOL AFWAL/AAAI-2	

## CONTENTS

	<u>Page</u>
1.0 Program Objective and SOW . . . . .	1
2.0 Executive Summary . . . . .	2
2.1 Overview . . . . .	2
2.2 LCTS Terminal Description . . . . .	2
2.3 LCTS Terminal Preparation . . . . .	3
2.4 LCTS Terminal Maintenance / Support . . . . .	3
2.5 LCTS Automatic Acquisition Upgrade . . . . .	4
3.0 Introduction . . . . .	5
4.0 Background . . . . .	5
5.0 LCTS Terminal . . . . .	6
5.1 Performance . . . . .	6
5.2 Description . . . . .	6
5.2.1 General . . . . .	11
5.2.2 Transceiver . . . . .	11
5.2.3 Servo Control . . . . .	16
5.2.4 Dual Mode Video Tracker . . . . .	22
6.0 LCTS Technical Performance . . . . .	31
6.1 Terminal Preparation . . . . .	31
6.2 Terminal Maintenance/Support . . . . .	32
6.3 Automatic Acquisition Upgrade . . . . .	35
6.3.1 Acquisition Description . . . . .	35
6.3.2 Acquisition Procedure . . . . .	36
6.3.3 Acquisition Logic . . . . .	36
6.3.4 Acquisition Implementation . . . . .	37
7.0 LCTS Technical Discussion . . . . .	40
7.1 Next Generation Auto-acquisition . . . . .	40
7.2 Comparison of Video to Quadrant Tracking . . . . .	45
Appendix A. Spiral Scan . . . . .	47
Appendix B. Dual Mode Tracker (DMT) Description . . . . .	51
Appendix C. Image Auto Tracker Algorithms . . . . .	61

## LIST OF FIGURES

<u>Figure</u>	<u>Title</u>	<u>Page</u>
5-1	Photograph of the Hughes laser communication terminal for the LCTS program. ....	8
5-2	Photograph of the Hughes gimballed transceiver for the LCTS program .....	9
5-3	Basic LCTS block diagram .....	12
5-4	Example of major system components of the LCTS system .....	13
5-5	Transmitter/receiver electronics block diagram .....	15
5-6	LCTS modem electronics. ....	17
5-7	Basic LCTS servo block diagram .....	18
5-8	LCTS terminal panel display .....	20
5-9	LCTS servo functional block diagram .....	21
5-10	Basic Dual Mode Tracker (DMT) block diagram .....	23
5-11	Dual Mode Tracker control panel .....	26
5-12	DMT control panel - acquisition mode .....	27
6-1	Acquisition logic flowchart - receiver .....	38
6-2	Acquisition logic flowchart - transmitter .....	39
6-3	Plot of angular commands for spiral scans of 3, 6, 9, and 12 degrees .....	41
6-4	Gimbal motion for 12-degree transmitter spiral scan (before potentiometer upgrade) .....	42
6-5	Gimbal motion for 12-degree transmitter spiral scan (after potentiometer upgrade) .....	43
6-6	Gimbal motion for 12-degree receiver spiral scan (after potentiometer upgrade) .....	44

LIST OF TABLES

<u>Table</u>	<u>Title</u>	<u>Page</u>
5-1	LCTS performance summary .....	7
5-2	LCTS weight and power summary .....	10
5-3	LCTS tracker control panel .....	28



Accession For	
NTIS GRA&I	<input checked="" type="checkbox"/>
DTIC TAB	<input type="checkbox"/>
Unannounced	<input type="checkbox"/>
Justification	
By	
Distribution/	
Availability Codes	
Dist	Avail and/or Special
A-1	

## 1. Program Objective and SOW

### 1.1 Objective

The objective of this program is to deliver Hughes-developed automatic tracking optical communication terminals to the Air Force in order to evaluate their performance for air-to-air communication applications.

### 1.2 Statement of Work

The contractor shall furnish two company-developed demonstration optical communications terminals for evaluation by cognizant government personnel. The two terminals shall be capable of demonstrating the basic features of voice and data communication, automatic active video spot tracking and pointing to the opposite terminal, and manual video-aided acquisition. The contractor will provide required on-site engineering support for maintenance and assistance to government personnel in evaluation of the system performance and verification of the system characteristics. The contractor shall provide an operator's instruction manual for use by government personnel during the test period.

The contractor shall develop an automatic scan algorithm which shall be incorporated into the optical communication terminals. The design goal is to cover an uncertainty of  $12^{\circ}$  azimuth x  $9^{\circ}$  elevation. The upgraded terminals shall be returned to AFWAL/AAAI for an additional 2-month evaluation.

## 2. Executive Summary

### 2.1 Overview

The Hughes Laser Communication Test System (LCTS) program has met the objectives of the Statement of Work within program target cost and with moderate schedule delay (considering the unforeseeable loss of two key personnel to the program). The LCTS program has established the basic viability of aircraft laser communication systems using GaAs laser diodes with video tracking/acquisition techniques. Video tracking and automatic acquisition were shown to provide a legitimate alternative to a quadrant detector approach (as used on HAVELACE). The LCTS terminals proved that a single subsystem, incorporating a CCD video camera, gyro-stabilized gimbal and servo electronics, can perform both automatic acquisition to 12-degrees field of regard and precision tracking to  $<100 \mu\text{rad}$  in support of aircraft laser communication.

In Air Force testing the LCTS terminals demonstrated automatic acquisition with handover to communication/tracking over the 5-mile range from the Bldg. 620 tower to a remote facility at Trebein. Both voice and data have been successfully transmitted over this 5-mile link. Air Force experiments have placed one terminal in a moving test van and demonstrated automatic tracking and communications in that hostile baseframe motion environment. Air Force testing is ongoing with the LCTS terminals and a summary report of the Air Force LCTS experiments is expected after testing is completed.

### 2.2 LCTS Terminal Description

The LCTS laser communication terminals were built by Hughes Aircraft Electro-Optical and Data Systems Group in the 1984 IRAD program. These terminals were intended to serve as proof-of principle prototype hardware to demonstrate the capability of current technology to support aircraft and ship laser communications applications. The low probability of intercept (LPI) and jam-resistant (JR) properties of laser communication systems offer potential advantages over conventional RF communication technologies for some important missions such as aircraft refueling and airborne command post computer data dump.

The LCTS terminals are two axis gimbal-mounted, gyro-stabilized transceivers which can support full duplex transmission at 19.2 Kbps (e.g., computer modem) data rates. A laser diode serves as the data transmitter and a PIN photodiode acts as the data receiver. Full automatic tracking capability is provided by a gimbal-mounted video camera with an off-gimbal micro-computer controlled video tracker. The microcomputer implementation of the video tracker allowed the straightforward addition of automatic acquisition for the LCTS program mostly in software. The closed loop tracking accuracy of the system is  $<100 \mu\text{rads}$ .

Separate optical apertures are used for transmit, receive, and tracking functions. Both terminals transmit and receive identical 905-nm wavelengths, which provides for ease of networking and manufacture, because separate transmit/receive apertures alleviate problems of self-jamming. A 1-inch optical aperture collects and collimates the laser diode output (100 Watts peak at 0.1 percent duty cycle) into a 0.5-degree beam. A 2.5-inch Cassegrain reflector (with a 10-nm background rejection filter) collects the received signal for a back-biased PIN photodiode communication detector, with about a 0.6 degree field of view.

The tracking detector is a MOS photodiode array with 384 x 485 pixels, and has its own 2.5-inch Cassegrain collector with 10-nm background filter. This video is digitized to six bits and processed by the video tracker to generate angular tracking signals. The video tracker can operate in centroid track or correlation track mode and is capable of automatically selecting the optimum mode. The angular error signals from the video tracker are sent to the servo electronics which then issues commands to the torque motors to change the gimbal angular position.

## 2.3 Terminal Preparation

Prior to initial shipment of the lasercom terminals for the LCTS program, several modifications were made to the terminals to add performance monitors for experiment data recording, facilitate ease of testing, and to ensure the required gimbal and transceiver performance.

Several performance monitors were added to the LCTS terminals, all of which were carefully implemented so as to not degrade performance by the process of measurement. Monitors were added to the transceivers to allow recording of outputs proportional to transmitted power level (with a fiber optic pickoff) and received power level (by monitoring received signal together with AGC voltage). Analog outputs were added to the servo to provide potentiometer measurements of gimbal angular position. The angular displays on the front panel were also calibrated. A detailed RS-232 video tracker interface was configured which provided a digital output proportional to angular tracking error as well as data on the various tracker states. Hughes assisted Avionics Lab personnel in development of the software to acquire the tracker outputs.

The Laser Diode Labs LDT-350 lasers in the transceivers were replaced with fresh lasers and the transmitter, receiver, and camera optics were then realigned. An experiment was performed with one of the old lasers which indicated it could support meteorological testing at 20 Kpps (20 Kbps with all "ones") for several minutes at a time before thermal effects caused the average power to drop significantly. A digital circuit was added to "and" the data and clock signals, which allowed the transceiver to operate with non-return-to-zero (NRZ) data waveforms. Neutral density filter sets were procured and measured for their transmission in the infrared, which were found to be slightly higher than the manufacturer's ratings in the visible spectrum. A mount was obtained so that the neutral density filters could be changed without removing the lens from the gimbal mount.

One gimbal's wiring was reworked to reduce friction, and both gimbals were rebalanced. Hall-effect sensors were added so that a signal was provided when the gimbal reach azimuth and elevation gimbal stops. A hinged rear panel was added to each terminal to provide easier access to hook/unhook the gimbal cable set. Two cable sets were fabricated which allow the gimbals to operate remotely up to 30 feet from the electronics rack.

An Instruction Manual for the LCTS terminals was prepared and delivered with the terminals. This document provides a description of the terminal hardware, performance, and operation as well as a discussion of the interfaces.

## 2.4 Terminal Maintenance/Support

Hughes provided almost 4 man-weeks of on-base technical support in one 2-man and three 1-man trips to WPAFB (Dayton). Initially, the LCTS program manager and an engineer arrived with the equipment and helped with equipment setup and operation. A video tracker card was damaged in shipping and returned to El Segundo for repair. Other than the tracker card, the terminals were found to be functioning properly, including the performance monitors. Close contact was maintained via telephone with the Air Force project monitor, during the periods without Hughes personnel on-base. The fiber-optic transmitter monitors were later upgraded on-base with 1000- $\mu$ m core fiber which had arrived, in order to improve the coupling coefficient.

Maintenance was provided to the terminal servo electronics, video tracker electronic cards and power supply electronics during Air Force testing. The video tracker cards were repaired individually on four-to-five occasions by shipment back to El Segundo, and all of the tracker boards had their grounding wires upgraded during the program. The power supplies were completely reworked and a recurring servo instability was eliminated during the automatic acquisition upgrade process. Additionally the calibration and stability of the angular position displays and outputs were improved during that time.

## 2.5 LCTS Automatic Acquisition Upgrade

The LCTS lasercom terminals include a microcomputer-based video tracker which provides the scan management and control for automatic acquisition. The microprocessor is capable of generating angular tracking commands to the servo electronics, and is under-utilized prior to automatic tracking. The acquisition function was added chiefly in tracker firmware except for the routing of a buffered potentiometer measurement of gimbal angular position to the tracker in order to close a first-order-position loop.

The center of the acquisition scan is designated by operator joystick control, and the scan is referenced to an angular position loop based on the gimbal potentiometer outputs. One terminal is designated as the acquisition transmitter and the other as acquisition receiver. (This is selectable on each terminal.) Each of the terminals performs a spiral scan for acquisition, with the transmitter scanning the entire scan field of regard (FOR) in the time it takes for the receiver to scan one acquisition cell. (A spiral scan is superior to a raster scan since it begins the scan at the most likely position of the target, enhancing the possibility of finding the target early in the scan pattern.) The scan tangential velocity is constant so that there is a constant dwell time per acquisition cell.

An acquisition cell is defined by the terminal beamwidth or field of view (FOV), as appropriate. For the acquisition transmitter, the number of acquisition cells is defined as the total scan FOR divided by the transmitter beamwidth. The present transmitting beamwidth is  $0.5^\circ$ , which can be treated as  $0.4^\circ$  to allow for beam overlap. In order to facilitate faster acquisition times, the number of acquisition cells for the acquisition receiver is given by the scan FOR divided by the video tracker FOV. Since the video tracker FOV is  $2.0^\circ \times 1.5^\circ$ , the larger FOV gives fewer acquisition cells which results in a shorter acquisition time. The acquisition receiver cell size is taken as  $1.4^\circ$  to allow for overlap. For both acquisition transmitter and receiver the dwell time per acquisition cell is  $1/30$  sec, which is one frame time for the video tracker.

The acquisition field of regard (FOR) is selectable between 3, 6, 9, and 12 degrees. The worst-case acquisition times are given by the receiver scan period plus one transmitter scan period plus one transmitter slow scan period. These worst case times are given by 1.1, 3.1, 10.0, and 27.3 minutes for 3, 6, 9, and 12 degrees, respectively (assuming the receiver does not miss the transmitter). Because the operator designates the center of the scan by joystick control, and by using a spiral scan, the expected value of the acquisition times should be much less than the above worst-case values.

### 3. Introduction

Optical communication systems for terrestrial, airborne and space jam-resistant (JR) and low probability of intercept (LPI) applications have become even more attractive and quite practical with the advent of the GaAs laser diode. Optical communication systems possess LPI properties due to the narrow beamwidth inherent with the laser source, and JR properties due to the narrow receiver spectral transmission and field of view. The possibility of a system with all-semiconductor optoelectronics offers several new features: very small size, low power consumption, long lifetime, and high reliability.

The GaAs laser diode has unique properties which make it attractive for use in an optical communication system. The laser resonator is a single monolithic structure of semiconductor crystal and is inherently mechanically stable. Other desirable properties include: (a) small size, (b) direct modulation of the optical emission by variation of the drive current, (c) single mode intensity profile and single wavelength optical emissions, (d) operation at a preselected wavelength within the spectral region of about 760 to 900 nm, and (e) the reliability features inherent in a semiconductor device. Direct modulation of the optical emission ( $> 1$  GHz) by the drive current eliminates the need for an optical pumping structure and separate optical modulator. A short current pulse, as would be used in a digital binary communication format, yields a corresponding laser light pulse.

A system which utilizes the GaAs laser diode as a primary laser source requires fewer optical and electro-optical elements than competing systems. The small size of the diode, usually 100 micrometer (height) x 300 micrometer (length) x 200 micrometer (width) is attractive since it reduces the size, weight, thermal and mechanical support requirements of the system. As a result of the small size, the laser drive circuit and laser diode may be miniaturized and mounted as a single integrated circuit. The smaller, simpler systems can be mounted on small gimbals, offering JR and LPI communication systems at useful data rates with minimum burden to the host aircraft.

### 4. Background

Hughes Aircraft Company Electro-Optical and Data Systems Group developed a prototype optical communication system during the 1983-1984 IRAD program which included the capability of optical voice and data transfer up to 19.2 Kbps, as well as video acquisition and automatic pointing/tracking of a distant receiver. This proof-of-concept optical communication system was designed to demonstrate that presently available optical communication technology is applicable to many DoD jam-resistant (JR) and low probability of intercept (LPI) missions, including aircraft format: n flying, aircraft refueling, and SAC airborne command post data dump.

The prototype Hughes lasercom terminals were discussed at the Military Communications Conference in Los Angeles in late October, 1984. The LPI GaAs laser diode system consists of two identical terminals with a selected wavelength of 905 nm (which is invisible to the human eye). Video lenses may be easily interchanged, and with minor modifications the system could incorporate different laser devices, transmitting beamwidths, or an avalanche photodiode receiving detector, for example. The system may be used for verification of basic communication links, characterization of point-to-point atmospheric propagation effects, and as a testbed for system design alternatives and future technology advances.

A basic system configuration has been successfully demonstrated at sea with the U.S. Navy between a shipboard terminal and a hand-held laser communicator manually pointed from a helicopter. Intermittent two-way communication was established, limited only by the ability to manually point the binocular unit from the helicopter. The manually pointed laser communicators have successfully demonstrated low probability of intercept communication between Naval vessels at ranges of about 8 to 10 nautical miles. Other testing of narrow beam (about 1.0 mrad) tripod-mounted terminals has shown greater than 20-mile range at sea level in a clear desert

atmosphere. At high altitudes (~30,000 feet), the predicted communications range would be greater than 100 miles with a narrow 1.0-mrad beam version of the current LCTS hardware.

## 5. LCTS Terminal

### 5.1 Performance

The LCTS terminal major performance characteristics include: (a) a beamwidth of about 0.5 degree, (b) a peak transmitted power of about 100 watts at 905 nm, (c) separate transmit, receive and track optics with diameters of 1.0 inches, 2.5 inches and 2.5 inches respectively, (d) an optical filter bandwidth of 10 nm centered at 905 nm, (e) receiver field of view of 0.6° and 2.0° x 1.5° for the communication detector and tracking array, respectively, (f) a track sensor sensitivity of about 30 pw per sensor element at 905 nm, (g) a tracking accuracy of <0.1 milliradians and (h) a signal-to-noise ratio in the PIN diode communication sensor of about 10 dB greater than that achieved before the recent improvements.

A performance summary of the prototype system is noted in Table 5-1. A photograph of one of the demonstration system terminals is shown in Figure 5-1, and a close-up photo of the gimbal assembly is shown in Figure 5-2. A recent test accomplished acquisition using the video camera display of the terminal line-of-sight (LOS), and with a manual scan of the terminal LOS using an operator joystick. A link was established between the company roofhouse and a helicopter at a range of 8 to 10 miles. This was beyond the visibility range with the unaided eye. As mentioned, Navy testing has been performed with both handheld and gimbal-mounted systems.

The weight and power of the prototype system components are summarized in Table 5-2. The system operates from the aircraft or normal ground power source and requires about 167 watts of prime power. The prototype LPI system has a component weight of about 53 pounds. A flight model is expected to weigh less than 40 pounds and require less than 150 watts of prime power.

### 5.2 Description

#### 5.2.1 General

Each optical communication testbed terminal is composed of five major components or subsystems. These include:

- (a) The optical transceiver portion consisting of the laser, its electronic driver, the optical detector and its preamplifier, the transmit and receive optics and the modulation/demodulation electronics
- (b) A two-axis gimbal used to point the laser transmitter based on error signals from the tracker - cooperative tracking is used with laser sources transmitting from each terminal to the other.
- (c) Gyro-stabilization and servo control electronics which isolate baseframe motion and convert the tracker error signal into gimbal drive signals which direct its line of sight to the proper angular direction
- (d) Acquisition and tracking electronics used to determine the angular error signal relative to the correct line of sight using video imagery and
- (e) A solid state acquisition and tracking area array sensor.

TABLE 5-1 LCTS PERFORMANCE SUMMARY

<u>ITEM</u>	<u>VALUE</u>
TRANSMISSION MODE	PULSED
LASER WAVELENGTH	905 NM
TRANSMIT BEAMWIDTH	0.5 DEGREES
TRANSMIT OPTICAL POWER	100 WATT PEAK POWER
RECEIVE FOV	0.6 DEGREES
TRACK FOV	2.0 x 1.5 DEGREES
RECEIVE SNR	>15 DB
DATA RATE	9600 bps, 19.2 Kbps*
OPERATING TEMPERATURE	0 TO +50°C
RANGE (CLEAR AIR AT SEA LEVEL)	8 - 10 MILES
AVAILABILITY	DAY OR NIGHT
ACQUISITION	OPERATOR INITIATED/ AUTOMATIC**
FIELD OF REGARD	$\pm 70^\circ$ AZ; $\pm 50^\circ$ EL
TRACK TYPE	CENTROID OR CORRELATION
TRACK RATE	$> \pm 70^\circ/\text{SEC}$ , AZ & EL $> \pm 100^\circ/\text{SEC}^2$ , AZ & EL
PACKAGING	4 FT, 19 INCH RACK
PRIMARY ELECTRICAL POWER	167 WATTS
WEIGHT	53 POUNDS

\* HIGHER DATA RATES AVAILABLE

\*\* AUTO ACQUISITION CURRENTLY UNDER TEST

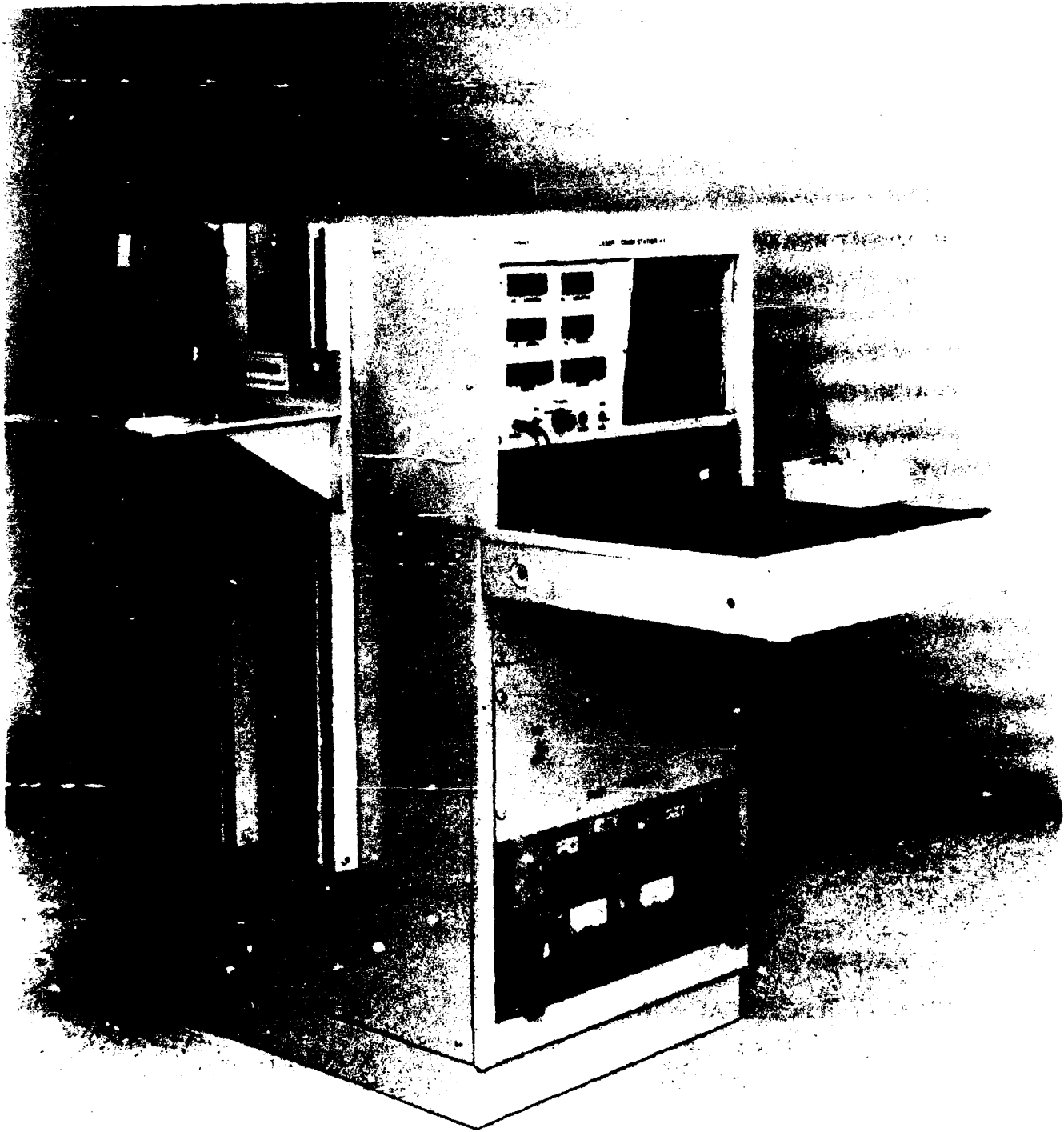


Figure 5-1. Photograph of the Hughes Laser Communication Terminal  
for the LCTS Program



Figure 5-2. Photograph of the Hughes Gimbaled Transceiver for the LCTS Program

TABLE 5-2 LCTS WEIGHT AND POWER SUMMARY

<u>COMPONENT</u>	<u>WEIGHT (LBS)</u>	<u>POWER (WATTS)</u>
• GIMBAL	6.7	N/A
• GIMBAL-BORNE OPTICS	6.3	1.0
• COMMUNICATION ELECTRONICS	0.8	10.0
• SERVO CONTROL ELECTRONICS	5.0	56.0
• TRACKER	24.6	90.0
• CABLING	2.0	N/A
• OPERATOR'S PANEL AND SUPPORT HARDWARE	7.5	10.0

A basic block diagram of the LCTS testbed is shown in Figure 5-3. Unlike other systems, all electro-optical components are mounted on-gimbal for simplicity. Separate apertures for the transmitter, communication detector, and tracking detector provide maximum photon collection capability and avoid self-jamming. The major components are shown in Figure 5-4.

The GaAs laser diode in the prototype system is operated pulsed so that digital binary coded data may be efficiently transferred from one terminal to the other. The data transfer capability of the current prototype LPI system is currently 19.2 kilobits per second with (equilike bit) digital data. Higher data rates to hundreds of megabits per second are available with other diode drivers. The laser diode employed in the prototype system is a M/A COM LDT-350 fiber-optic-coupled multi-spatial mode diode array collimated to a far field beam divergence of about 0.5 degrees. It is operated at a peak optical power level of about 100 watts, and duty cycle less than or equal to 0.1 percent.

Separate transmit and receive optics are used in order to achieve the high degree of transmit-to-receive isolation required (as much as 90 dB). Additionally, this avoids self-jamming and enables a single laser wavelength to be transmitted simultaneously between any two terminals. Identical, modular, cost effective terminals are inherent with this approach. A small refractive telescope with a diameter of 1 inch is used as the transmit antenna. A slightly larger reflective telescope with a diameter of about 2.5 inches is used as the communication receive antenna. The field of view of the receive telescope is about 0.6 degrees. The incident laser light from the opposite terminal is collected by the receive optics and routed to a solid state EG&G FND100 PIN diode detector. The receiver optics incorporate a narrow bandwidth optical filter (about 10 nm) in order to exclude unwanted background light and efficiently transmit the incident laser light. Night or daylight operation with the sun near the field of view is available.

A third 2.5-inch diameter telescope is used to route light to a solid state tracking sensor which is sensitive to both visible and 905-nm radiation. The solid state tracking sensor is a silicon multielement area array with a field of view of about 2.0°. The array provides a video signal to an off-gimbal video tracker which, in turn, provides the line of sight azimuth and elevation errors to the off-gimbal servo control electronics. The two axis gimbal is gyro-stabilized so that the line of sight pointing error achieved with this video tracking concept is less than 0.01 milliradians.

The video tracker is operable as a laser spot tracker, termed centroid tracking, as well as image correlation tracking. In centroid mode, the system tracks the bright laser spot on a dark background. In correlation mode, the system tracks on some selected geometrical contrast features within the image of the opposite terminal. The video tracker is a version of the Hughes modular tracker line. The servo control electronics and the video tracker electronics were originally developed for other applications and adapted to this new function. These electronic components may be placed about 30 feet remote from the gimbal.

## 5.2.2 Transceiver

### 5.2.2.1 General

The laser communication transceivers consist of the modulation electronics, laser diode driver, GaAs laser diode, transmitting optics, receiver collecting optics, EG&G PIN diode detector, preamplifier, and demodulation electronics. The LCTS terminals basically integrate existing handheld laser communication receivers into a gyro-stabilized gimbal assembly with automatic video tracking. The M/A COM LDT-350 transmitter laser diode is a multi-spatial mode fiber-optic coupled array with a peak power capability of 100 watts at 0.1-percent duty cycle.

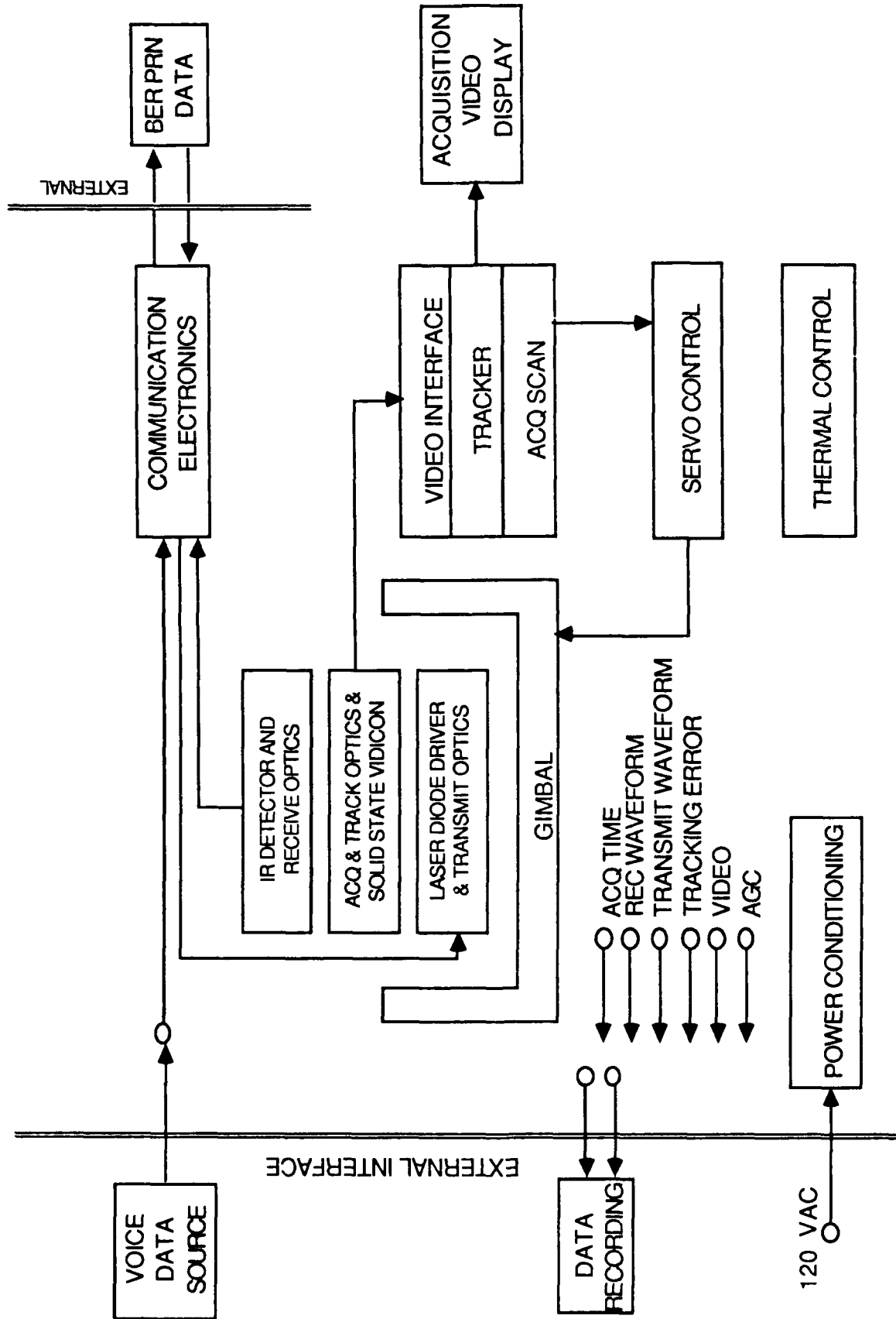


**FIGURE 5-3 BASIC LCTS BLOCK DIAGRAM**

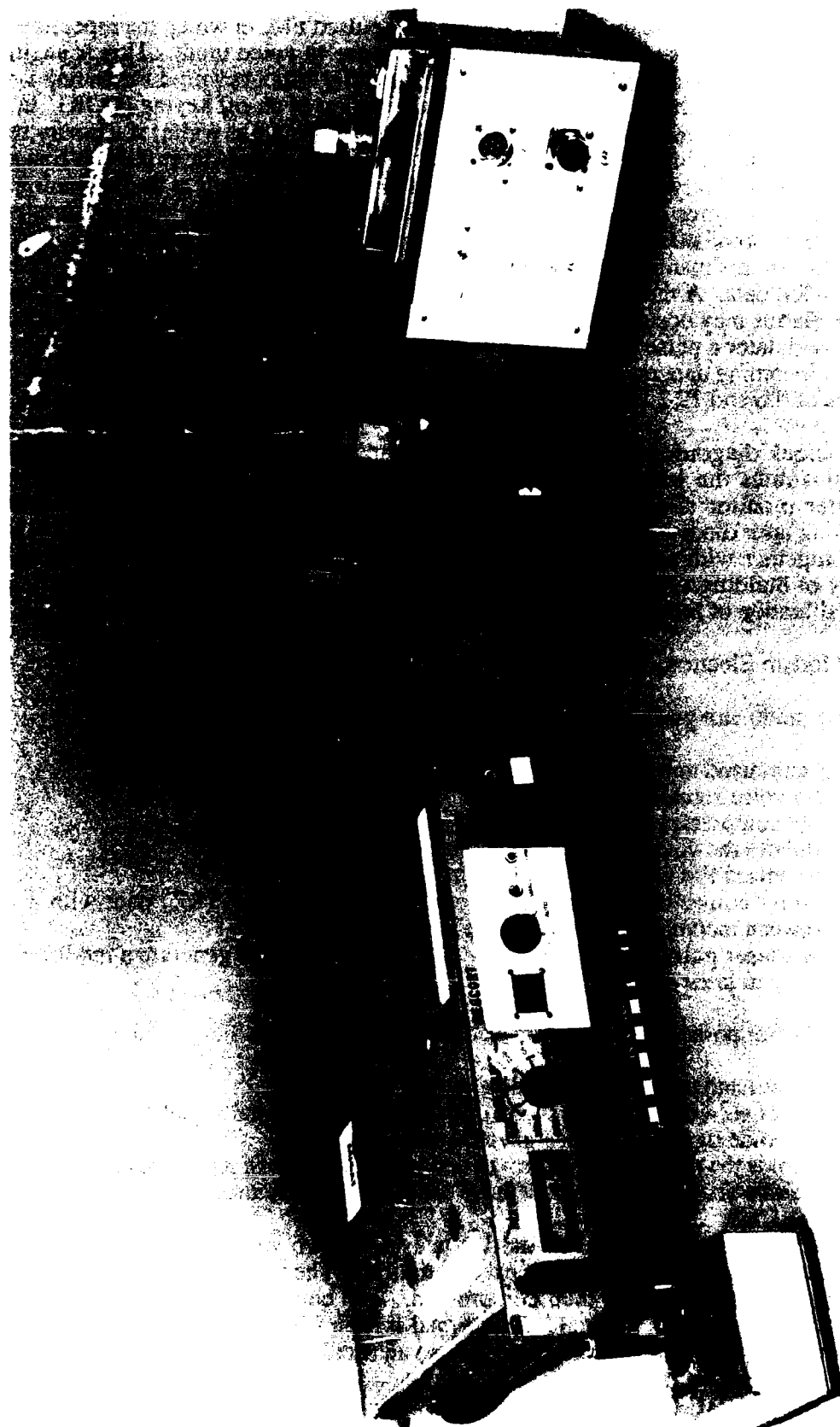


Figure 5-4. Example of Major System Components of the LCTS System

For analog voice the modulation format uses pulsed FM, in which the repetition frequency of a periodic pulse train is analog modulated in response to voice input. This is analogous to CW frequency modulation in that laser diode power linearity is not required for analog voice linearity. For data transmission the modulation format is a variation of on-off keying (OOK). In conventional OOK, a laser pulse is transmitted in a time slot (equal to the pulse width) if a binary one is present, and no laser pulse for binary zero. In the LCTS terminals a narrow laser pulse is transmitted on the transition from a binary zero to one, so that a laser pulse is emitted at the beginning of each data pulse. In order to force a positive-going transition to trigger the laser pulse for non-return-to-zero data, the data modulator performs the logical "and" operation between the incoming data and an input clock. In this manner, a narrow laser pulse is transmitted at the beginning of each data pulse even for NRZ data. A threshold for pulse detection of the received waveform is chosen to reflect that false alarms may occur more readily than for conventional OOK. When threshold is exceeded at the demodulator a pulse is triggered by a one-shot circuit which has an adjustable pulse width to match the incoming data rate. In the LCTS system, pulse widths of 104 and 52 msec correspond to data rates of 9.6 and 19.2 kbps. The pulse widths are adjustable  $\pm 2$  msec.

A block diagram of the communication transmitter and receiver is shown in Figure 5-5, which illustrates the location of the transmit/receive performance monitors. The fiber optic transmitter monitor allows calibrated reproduction of the pulsed optical waveform from the transmitting laser diode. The received optical waveform is characterized by the post-AGC amplifier pick-off together with an output indicating the value of gain in the AGC circuit. This avoids the necessity of building a second ultra-wide dynamic range or logarithmic amplifier chain, and still allows calibration of receiver responsivity.

#### 5.2.2.2 Modem Electronics

The modulator portion of the modem electronics:

- a) Accepts command to be in voice or data mode
- b) Amplifies voice signal from microphone
- c) Filters and compresses the voice signal
- d) FM modulates the voice carrier
- e) Develops pulsed FM analog signal
- f) Or, converts non-return-to-zero (NRZ) data to return-to-zero (RZ) data with a logical "and" function between incoming data and a clock input
- g) Triggers a laser pulse based on a positive-going transition to generate a modified OOK digital signal to apply to laser driver.

The demodulator portion of the modem electronics:

- a) Accepts command to be in voice or data mode
- b) Demodulates pulsed FM analog signal or modified OOK digital signal
- c) Amplifies voice signal for application to headset or speaker
- d) Or, thresholds the detected waveform to detect the presence of a laser pulse
- e) Triggers a one-shot to output a data pulse for each threshold crossing.

Functionally, the modem board consists of two oscillators, two low-pass filters, a microphone amplifier and an audio speaker amplifier. The incoming analog voice signal from the microphone is amplified and then compressed. The compression is used in the event that the incoming volume level is too high. This signal is then filtered to remove frequencies outside the voice band. The filtered signal is then applied to an oscillator that is FM modulated. The amplitude

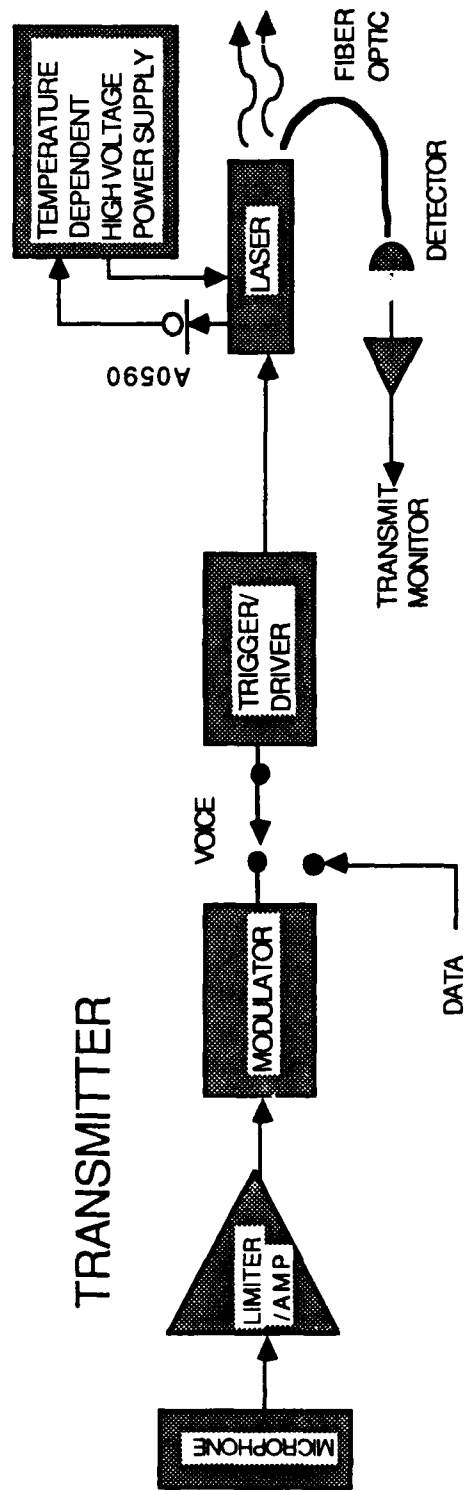
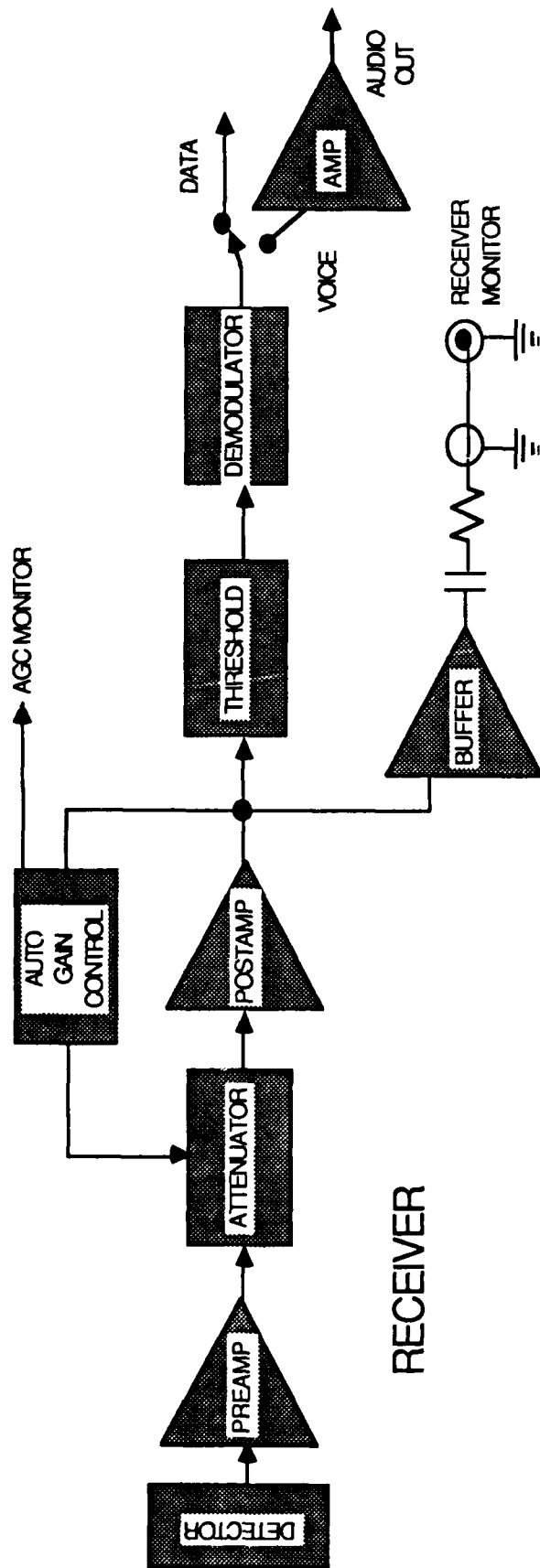


FIGURE 5-5. TRANSMITTER / RECEIVER ELECTRONICS BLOCK DIAGRAM

of the incoming signal is set such that the oscillator is only modulated  $\pm 10$  percent. The modulated signal is then applied to a pulse shaper that controls the pulse width of the laser.

The second half of the modem board demodulates the received signal. The signal that comes from the receiver board is interfaced to a tracking oscillator that replaces any missing pulses sensed by the receiver, to minimize the audio distortion. The tracking oscillator output is fed into the low pass filter input which strips off the carrier and leaves the audio intact. The audio signal that comes out of the low pass filter is fed into a low voltage audio power amplifier. The output from the power amplifier can drive a headset and/or an 8-ohm speaker.

Another feature that is designed into the modem board is the data switch. This is an electronic switch that shuts off analog voice mode (the two oscillators) and will allow outside data to be fed directly to the pulse shaper of the laser driver. The data that is received from the IR link is fed out of the modem board and is then ready for decoding. The data that is received (when in the data mode) bypasses the demodulator and the audio output, and goes directly to the data decoder. The transceiver has nominal data rates of 9.6 or 19.2 Kbps with pulse widths of 104 and 52 msec, respectively. The pulse widths can be adjusted  $\pm 2$  msec. The physical layout of controls for the modem electronics boxes is shown in Figure 5-6, which also identifies the pin configurations on the connectors.

### 5.2.3 Servo Control

#### 5.2.3.1 Introduction

The servo controls for the LCTS provide the means by which a gimbal with camera and laser transmitter/receiver are pointed and stabilized around a line of sight. The servo controls are comprised of a gimbal assembly, servo electronics assembly, and a display and command assembly.

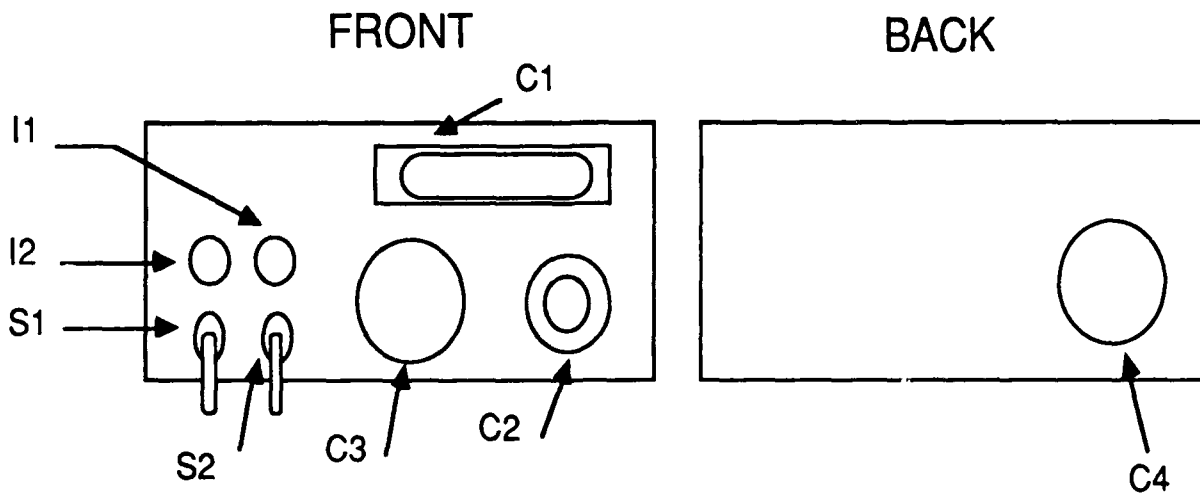
Interface with a dual mode video tracker (DMT) provides the servo controls with a means to servo the gimbal assembly around a given target. With the target being a second LCTS, communication is possible once the second LCTS also locks into track mode on its target LCTS.

#### 5.2.3.2 Summary of Operation

A basic servo block diagram for the LCTS system is shown in Figure 5-7. The line-of-sight (LOS) stabilized gimbal is pointed in azimuth and elevation to desired angles via a two-axis joystick. The joystick command is processed by a dual mode optical tracker (DMT) which provides rate commands to the gimbal AZ and EL torquers. An operator, viewing the video display of the camera field of view (FOV) searches for the desired target for communication. Once the target is spotted, depression of the joystick end switch will hand over gimbal commands to the DMT and the derived target optical angular errors. These errors are input into the servo electronics as rate commands to the gyro torquer motor of each axis, respectively. Each axis correspondingly drives the gimbal to alter the LOS angles to null out the gyro torque (and hence track error) commands.

#### 5.2.3.3 Servo Description

The servos used for LCTS are composed of a tracker-controlled loop and an inner stabilization loop for each of the two servo axes. The stabilization servo loops use gyros to sense gimbal motion in order to remove baseframe disturbances with respect to the gyro inertial reference. The tracker outer loops either provides feedback from image LOS track errors or open-loop rate



## LEGEND

- I1 POWER ON INDICATOR -LED
- I2 SIGNAL ACQ INDICATOR-LED
- S1 SWITCH -POWER ON
- S2 SWITCH - 9.6/19.2 BAUD RATE
- C1 DATA COMM CONNECTOR  
25- PIN D MALE  
(AD1B-1S-25)
- C2 AUDIO IN CONNECTOR  
3 LEAD MALE HEADPHONE
- C3 SYSTEM INPUT  
8-PIN CIRCULAR MALE  
(MS3470L12-8P)
- C4 SYSTEM OUTPUT (TO GIMBAL)  
8-PIN CIRCULAR MALE  
(MS3470L12-8P)

## CONN PIN WIRE FUNCTION

CONN	PIN	WIRE	FUNCTION
C1	1		GND (SHIELD)
C1	2		INPUT (DATA IN)
C1	3		OUTPUT (DATA OUT)
C1	7		GND
C1	13		DATA ENABLE (ACTIVE LOW)
C1	24		CLOCK IN
C1	25		SUPPLY +6V OUT
C2		BLACK	GND
C2		YELLOW	MIKE INPUT
C2		WHITE	EARPHONE
C3	A	BLACK	GND
C3	B	GREEN	LASER POWER
C3	C	WHITE	DATA CTRL
C3	D	NC	
C3	E	BLUE	DATA OUT
C3	F	YELLOW	DATA IN
C3	G	RED	+6 V REG OUTPUT
C3	H	RED	VCC
C4	A	NC	
C4	B	WHITE	DATA OUT 1
C4	C	GREEN	DATA OUT 2
C4	D	RED	VCC (FROM C3-H)
C4	E	BLUE	REC DATA IN 2
C4	F	WHITE	REC DATA IN 1
C4	G	NC	
C4	H	BLACK	GND

FIGURE 5-6. LCTS MODEM ELECTRONICS

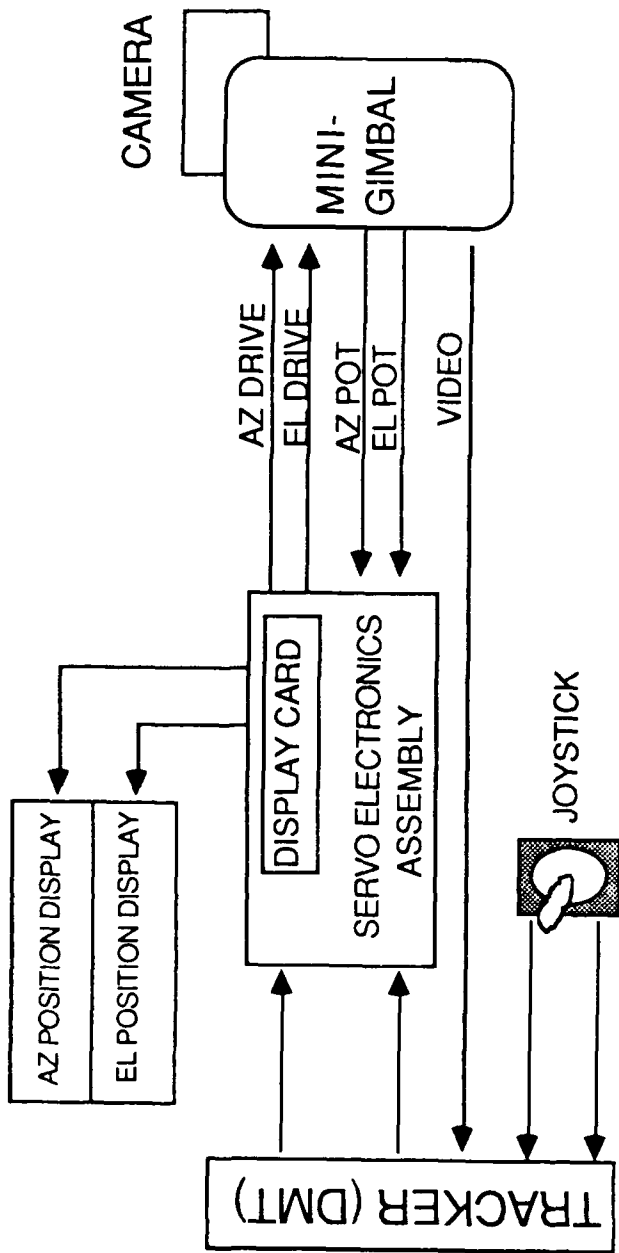


FIGURE 5-7. BASIC LCTS SERVO ELECTRONICS BLOCK DIAGRAM

commands via joystick.

#### 5.2.3.4 Stabilization Loop

The two gimbal servos are each of the type-II lead-compensated variety. Servo loop bandwidths are approximately 20 Hz with 40° phase margin. The servo loops each use a single-axis rate integrating gyro as the L.O.S. feedback sensor for each particular axis. Outside these loops are low-frequency (6 Hz) type-I track loops (when in track mode).

#### 5.2.3.5 Track Loop

Once depressed, the joystick button toggles the mode of the outer loop of each servo axis. The outer loop either is in track or in command (man in loop) mode. As a track loop, the tracker-unit-supplied LOS errors drive the gyro torquers to keep the target image centered in the FOV.

#### 5.2.3.6 Hardware Description

Each LCTS terminal contains servo control hardware consisting of a servo electronics assembly or card cage, a mini-gimbal assembly, a display/command interface electronics and panel, a dual-mode tracker (DMT) and power supply assembly. Both power supply and servo electronics assemblies are resident at the rear of each LCTS terminal with a DMT tracker power supply assembly. As shown in the panel display in Figure 5-8, the angle displays are 3 1/2-digit digital LED displays which indicate Azimuth and Elevation of the inner gimbal relative to boresight. These displays are scaled in degrees as sensed by the gimbal angle potentiometers.

The 4 1/2 counter display for Acquisition time display/measurement provides a means of displaying time required to acquire a target. This can be manually or (if connected to a TTL trigger) automatically started and stopped. The display/command interface and panel is at the front portion of the LCTS and provides the functions of servo power on/off, gimbal angular position display, acquisition time measurement/control, and gimbal limit indication. Additionally, a video monitor and headset communication interface are resident on the LCTS front panel. A joystick angular rate command control is provided on the DMT tracker interface horizontal panel.

Each gimbal is tethered to the LCTS station via its interface cable. The gimbal contains two gyros, two rotary torquers, two angle-sensing conductive plastic potentiometers, and angle limit sensing hall-effect sensors. Additionally, a video tracking camera, laser transmitter, and laser receiver are resident on the inner-gimbal L.O.S. stabilized portion of the gimbal.

The servo electronics card chassis located at the console rear houses six cards. As shown in the servo functional diagram of Figure 5-9, these cards (A1-A6) form the essential elements for controlling the two gimbal servos. Azimuth and Elevation servos each require two cards (an amplifier and a loop compensation card) for processing gyro, potentiometer, and track commands. The electronics is completely analog and can be packaged into a significantly smaller package in production. The amplifiers (A5 + A6) each provide up to 5 amps of current to the respective torquer motor.

A gyro spin motor drive board (A1) provides both a 900-Hz spin motor sinusoid and a 19.2-kHz gyro excitation sinusoid for detection of LOS motion in that axis. A second card (A2) provides current amplification to drive both gyro spin motors simultaneously. Power requirements (typically less than 10 watts) for the servo are met by the DC power supply at the rear of the LCTS.

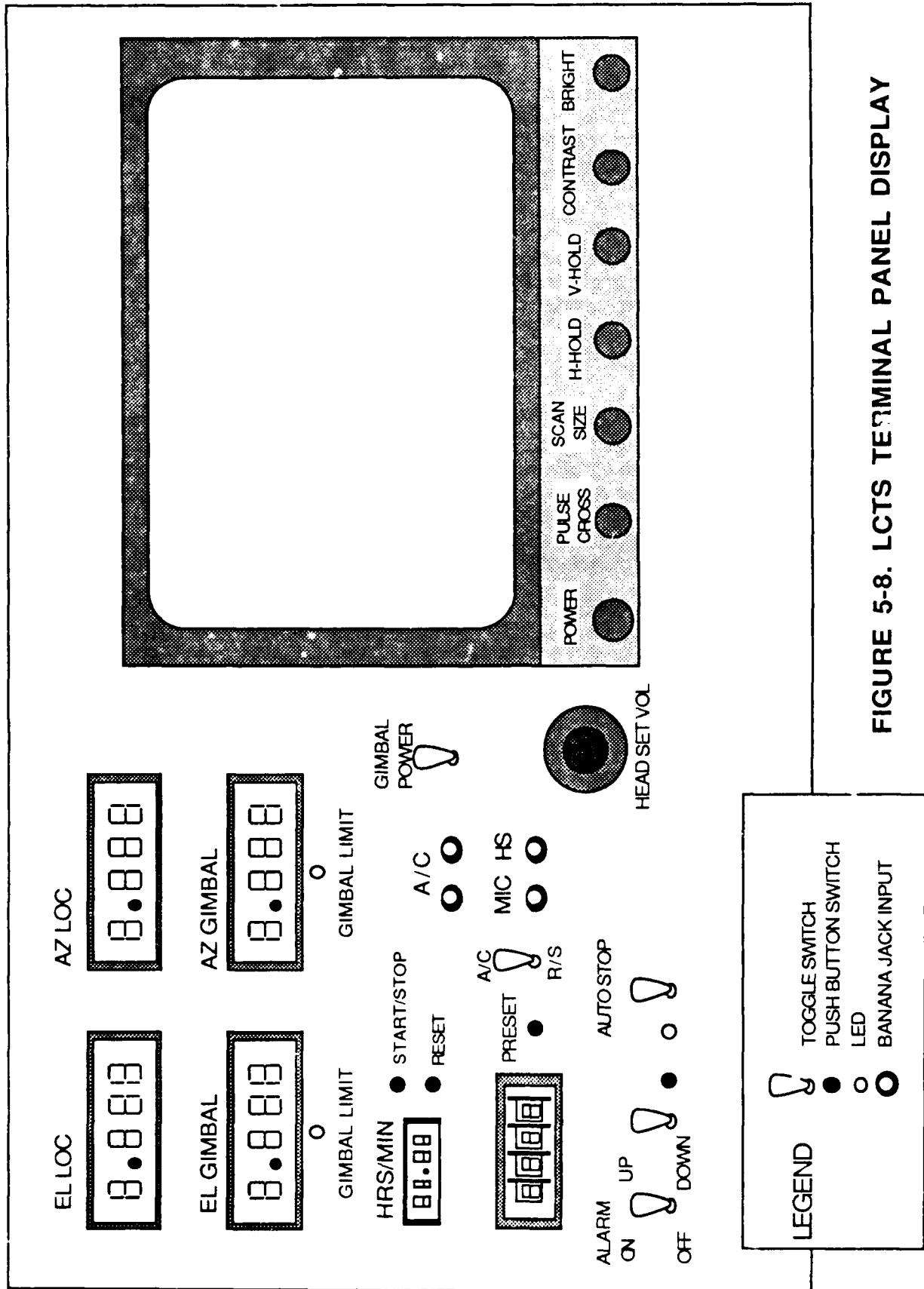


FIGURE 5-8. LCTS TERMINAL PANEL DISPLAY

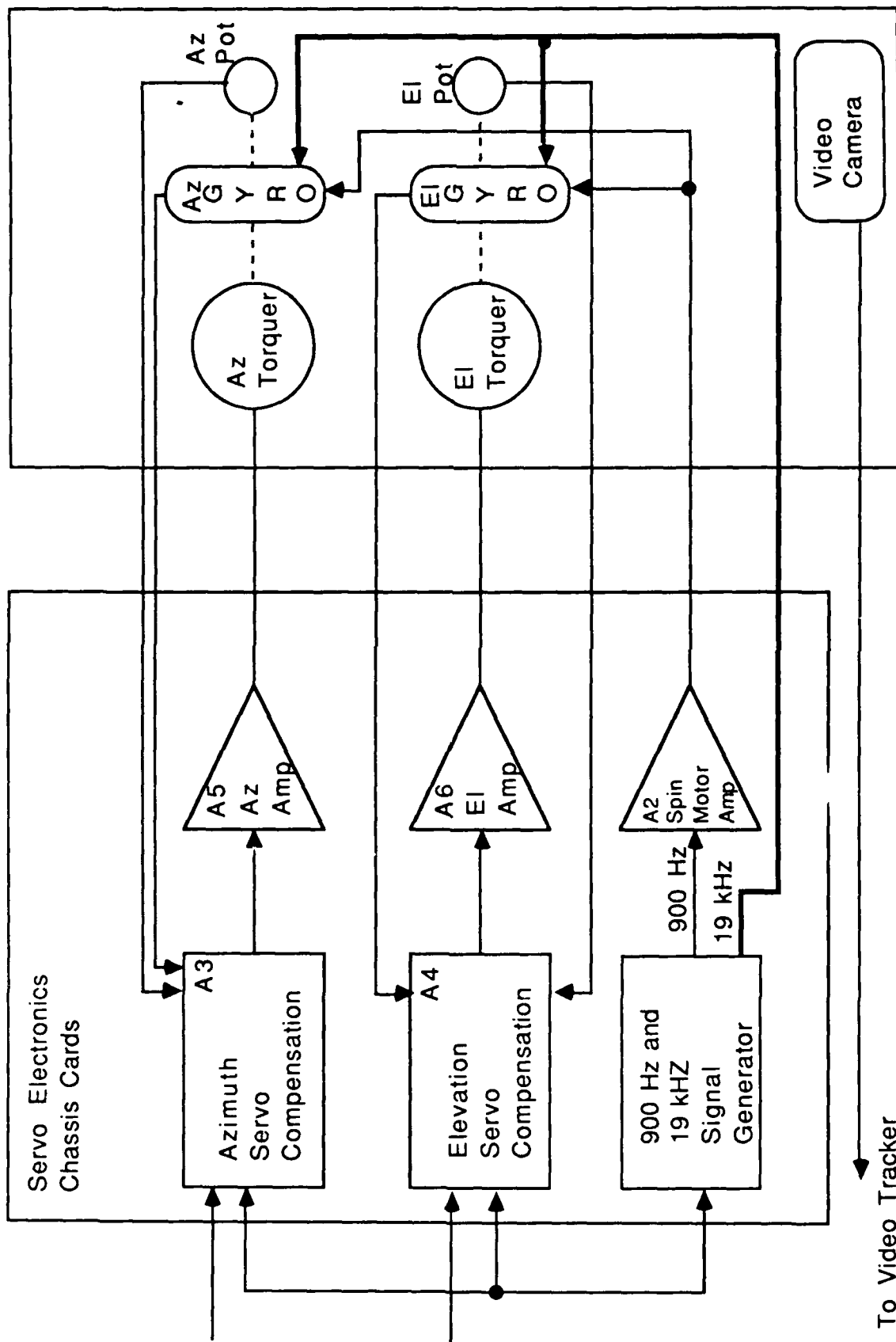


FIGURE 5-9. LCTS SERVO FUNCTIONAL BLOCK DIAGRAM (TRACK LOOP NOT SHOWN)

The power supply provides +24v to be used to power the electronics and gimbal assembly. A 12-volt supply is used to provide video camera power. Servo power is controlled by a switch at the front of the LCTS while console power is controlled by a switch at the LCTS console rear. The console requires 117VAC, 60 Hz for operation.

#### 5.2.4 Dual Mode Video Tracker

This section describes the basic dual-mode video tracker (DMT) for the LCTS terminals. Additional description of the DMT is provided in Appendix B and a discussion of image auto-tracker algorithms is provided in Appendix C.

##### 5.2.4.1 Introduction

The LCTS tracker is based on the Hughes dual-mode video tracker (DMT). The DMT electronically processes video signals to generate track errors. The track error signals describe the scene-to-scene motion of the object of interest or target. These errors are used to drive the pointing system upon which the video sensor is mounted and thus track the target.

Figure 5-10 is a top-level block diagram of the DMT unit and its application in the laser communication terminal. It comprises four major subsystems: the video preprocessor, the centroid error processor, the correlation error processor and the microcomputer. The function of the video preprocessor is mainly to convert the analog sensor video to digital form for the error processors. The microcomputer is the DMT controller. It performs all of the low rate data computations, automatic algorithms, and controls the interfaces with the external world. The centroid and correlation error processors are hardwired signal processors which perform many operations for every pixel. They generate the raw data required by the microcomputer for final computation of the centroid and correlation track errors. Two types of error processors (hence "dual" mode) are used because each has its own strengths and weaknesses depending on the type of video scene that is being processed. The inclusion of both types of error processors allows the DMT microcomputer to dynamically select errors from the processor that is the better performer. As with all automatic DMT functions, this selection may be manually overridden if desired.

##### 5.2.4.2. Video Format

The DMT was designed to accommodate a wide variety of video sensors from standard TV cameras to FLIR type sensors. The video camera used in the LCTS system produces a standard TV signal with 525 lines/frame, two (60Hz) vertically interlaced fields per frame. The input to the DMT is a composite video signal from which the DMT strips a composite sync. The DMT phase-locks a pixel clock to this composite sync. The LCTS pixel clock is approximately 5.7Mhz and yields 320 pixels in the active portion of a video line.

##### 5.2.4.3. DMT Functions

###### Video Preprocessor

The DMT's video preprocessor serves as the analog front-end for the predominantly digital DMT. Before digitization the analog video signal is processed so as to enhance the contrast of the tracked target. The video preprocessor contains automatic video level (offset) and gain stages which, under control of the DMT microcomputer, can stretch the video signal so that it covers the full range of the video A/D. The DMT video preprocessor digitizes the stretched analog signal to 6 bits.

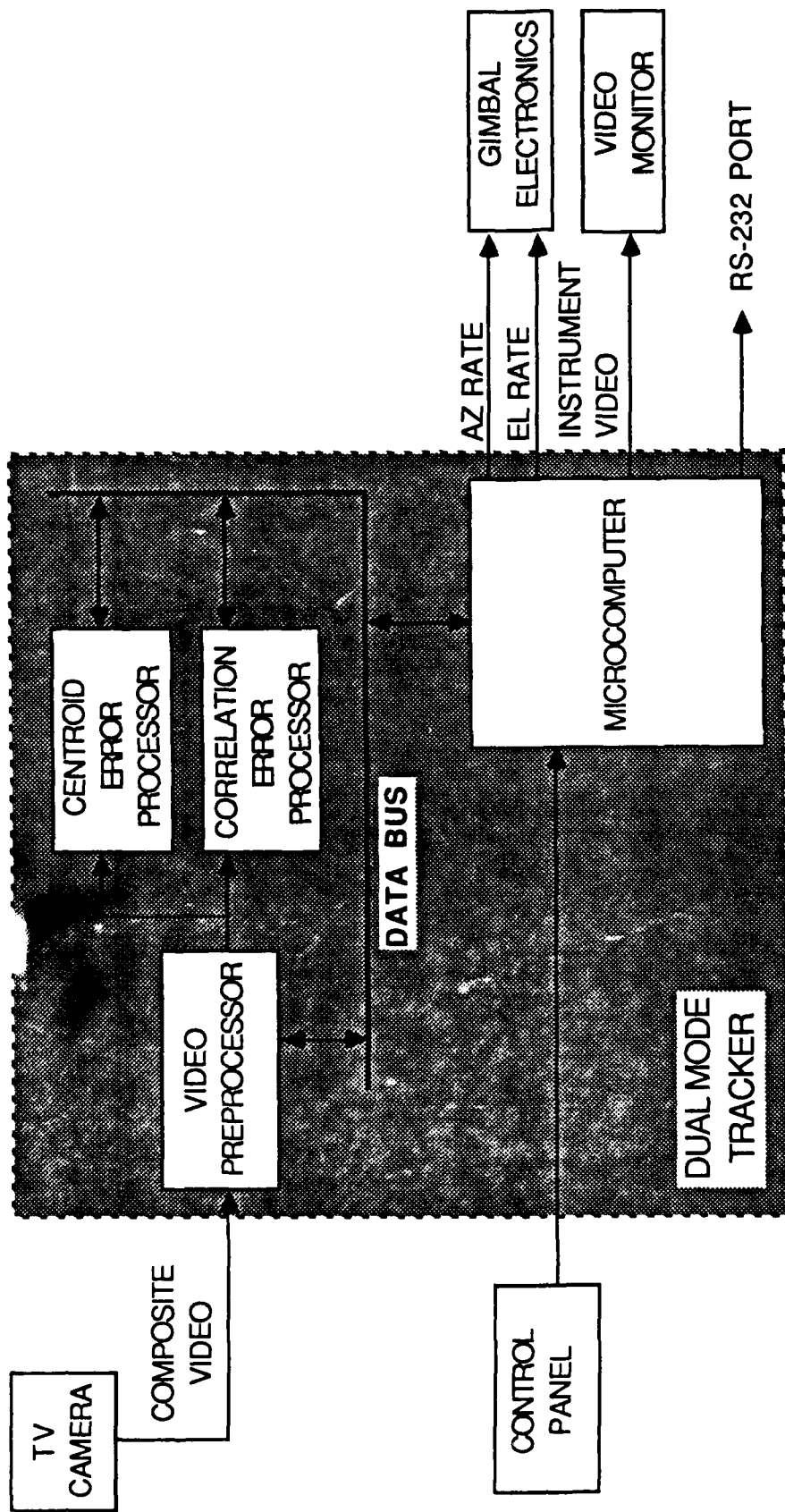


**FIGURE 5-10. BASIC DUAL MODE TRACKER BLOCK DIAGRAM**

### Centroid Error Processor

The centroid error processor is the simplest of the two types of error processors in the DMT. In order to generate a centroid error a portion or all of a target must be able to be thresholded or separated from its surroundings by virtue of its video intensity being either greater (positive contrast) or less (negative contrast) than the intensity of its immediate background. The thresholded video signal represents pixels which are assumed to be part of the target and their centroid can be easily computed. The DMT's centroid processor is a 1-bit centroid process (i.e., all thresholded pixels are weighted equally regardless of the degree they exceed threshold). The contrast as well as the threshold can be automatically determined by the DMT microcomputer based on target and background intensity histograms generated by the centroid error processor. This intensity histogram data is also used to determine the track status of the centroid processor and detect an impending break-lock condition. The centroid error is computed only within a target gate or window area. The DMT centroid error processor also determines the edges of centroid video within the track gate. This information is used by the microcomputer to automatically size the centroid track gate.

### Correlation Error Processor

The correlation error processor entails much more signal processing than that required of the centroid processor. Only a brief description of the correlation error process is given here. The incoming video is recursively filtered and stored in a reference memory. For a given pixel in the input scene an azimuth and elevation gradient is generated by subtracting the two pixels to the left and right or top and bottom of the given pixel. These gradients are multiplied by the difference between the given input pixel intensity and its corresponding pixel intensity in the reference memory and the products are accumulated over the track gate area. These accumulated correlation values and others are finally used by the DMT microcomputer to compute the correlation error.

A unique feature of the DMT's correlation error processing is the continuous updating of the reference memory. The DMT microcomputer can automatically control the time-constant of the reference memory filter based on the magnitude of the computed errors so as to adapt the reference update rate to the scene dynamics.

The error processor function also produces information used by the DMT microcomputer to automatically size the correlation track gate and determine the correlation track status.

### Microcomputer

The DMT microcomputer is based on a general purpose microprocessor. It supports the functions of the other three functional blocks and controls the DMT external interfaces. A majority of its processing deals with the automatic functions of the video preprocessor and the error processors. Its major tasks by DMT functional block are:

#### VP

- 1) Automatic level control
- 2) Automatic gain control.

#### CENTROID

- 1) Error computation
- 2) Contrast and threshold
- 3) Gate size
- 4) Track status.

### CORRELATION

- 1) Error computation
- 2) Reference memory time-constant
- 3) Gate size
- 4) Track status.

### GENERAL

- 1) Automatic track mode (centroid/correlation)
- 2) Track Loop Compensation
- 3) External command interface (control panel)
- 4) Instrumentation data interface.

#### 5.2.4.4. Operator Controls

Figure 5-11 illustrates the LCTS DMT tracker controls. In general a means has been provided for manually overriding all the automatic mode control operations of the DMT. For the majority of tracking runs, the DMT may be operated in its default state with all automatic mode control functions enabled. The most common manual override used by the operator is that of track mode (centroid or correlation). The operator may know the type of scenes being tracked and desire to select a particular track mode. In general, correlation works best for extended targets (larger than 5 pixels) and can perform well on relatively low signal-to-noise ratio (SNR), low contrast scenes. Centroid works well on small targets but requires a scene with a good SNR and sufficient contrast to allow the target to be thresholded. The DMT control panel as modified for acquisition mode is shown in Figure 5-12.

A typical track run begins with the operator manually tracking the target of interest on the video monitor. The gimbal is controlled by the rate stick so that the target appears under the cross-hair symbols on the video screen. Automatic tracking is then initiated by pressing the button on top of the rate stick. If operating in auto gate size mode, the error processor gate symbols will not appear on the video monitor until after track has been initiated. The correlation error processor's gate symbol appears as a solid-line box outlining the processing area, while the centroid symbol is made up of dashed-lines. Once track has been initiated, the DMT will continue to attempt to track the target until the operator terminates track by pressing the rate stick button again. When automatic tracking has been terminated, the operator again has control of the gimbal via the rate stick. Table 5-3 describes each panel control and its function.

#### 5.2.4.5. External Serial Interface

The LaserCom DMT microcomputer will output the active gate's track errors and certain tracker status bits each video field through its RS-232C port. The tracker interface is described in detail in the LCTS Instruction Manual.

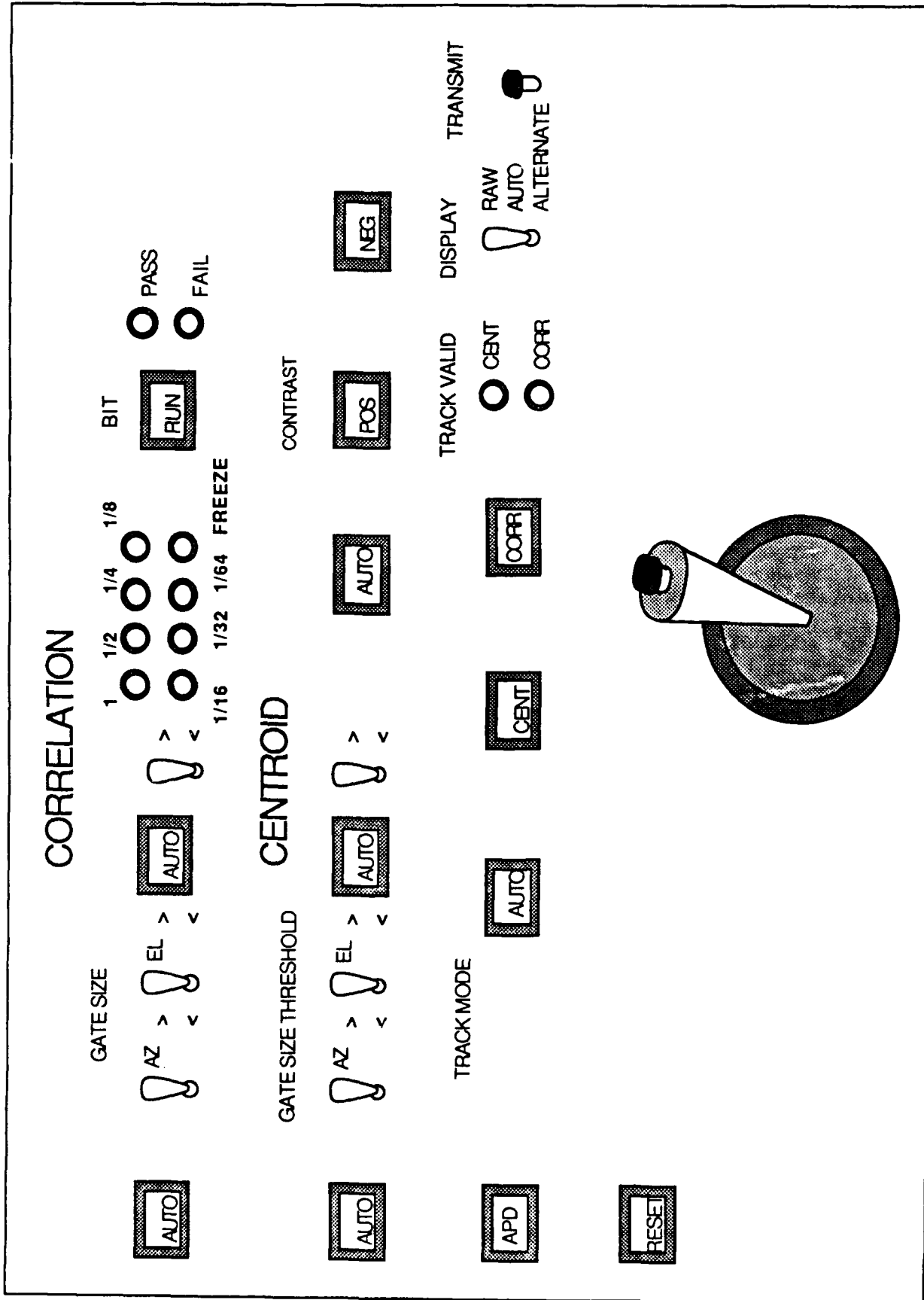


FIGURE 5-11. DUAL MODE TRACKER CONTROL PANEL

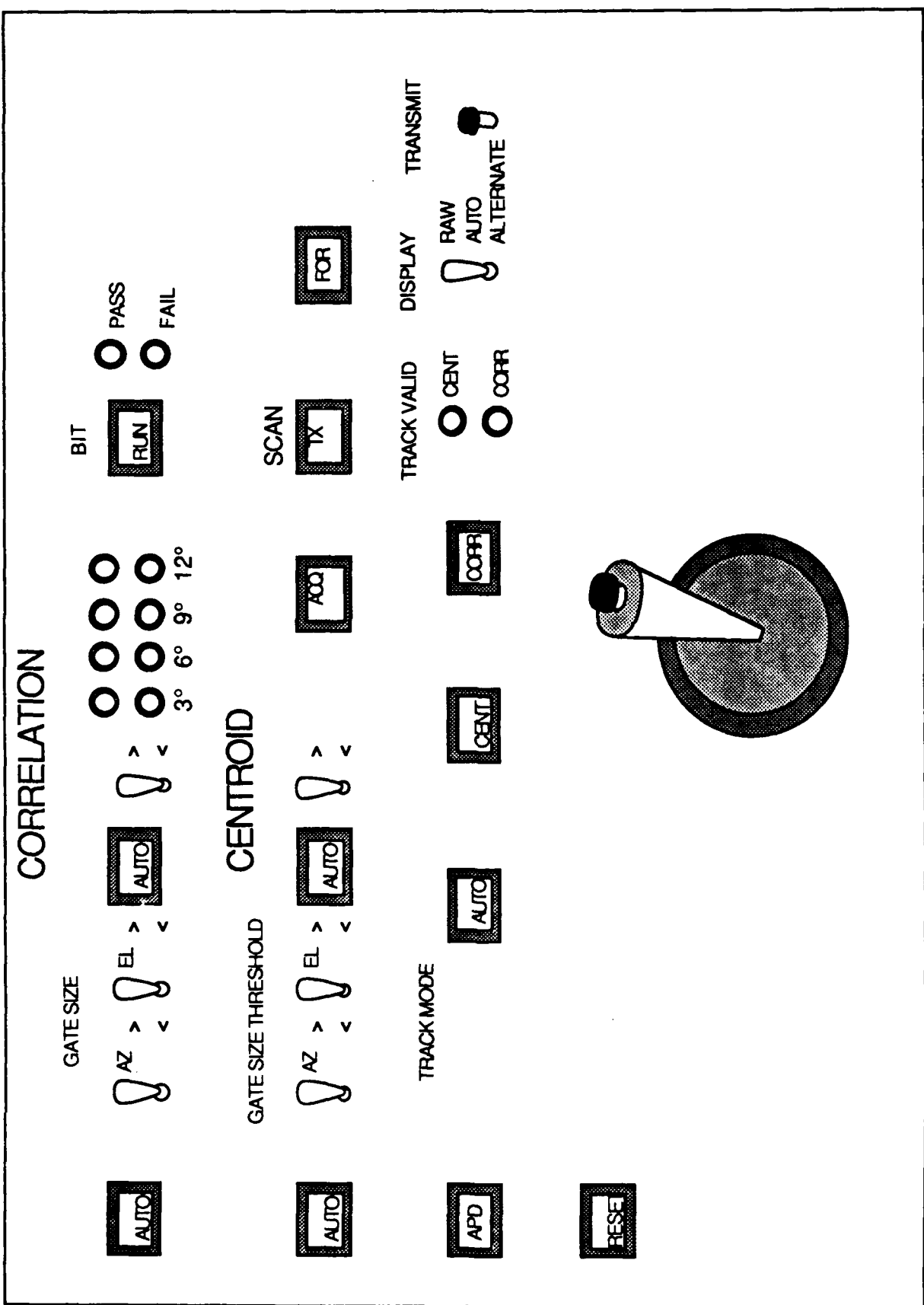


FIGURE 5-12. DMT CONTROL PANEL -ACQUISITION MODE

Table 5-3 LCTS Tracker Control Panel

<u>CONTROL NAME</u>	<u>DESCRIPTION</u>
<u>Correlation Tracker</u>	
Gate Size, Auto	Lighted pushbutton which toggles between automatic and manual correlation gate size. The tracker must be in a manual track mode in order to select manual gate size. Button is lit in AUTO gate size mode.
Gate Size, Az., El. toggles	Two spring-loaded toggle switches which increase or decrease the gate size when in manual gate size mode. Push the switch up to increase the size and down to decrease.
W1, Auto	Lighted pushbutton which toggles between automatic and manual correlation reference memory filter coefficient (W1) control. Button is lit in AUTO mode.
W1,toggle	Toggle switch which cycles through the selection of the correlation W1 values.
W1, LEDs	Eight LEDs which indicate the current setting of the correlation W1 value in either W1 automatic or manual modes. The possible values for W1 are 1, 1/2, 1/4, 1/8, 1/16, 1/32, 1/64, and freeze. When W1 is set to "freeze" the present reference memory is frozen and the incoming scene is ignored. When W1 equals one the reference memory is continuously set equal to the incoming scene. For the other values of W1, the new reference memory is set equal to the incoming scene times W1 plus (1-W1) times the old reference memory value.
<u>Centroid Tracker</u>	
Gate Size, Auto	Lighted pushbutton which toggles between automatic and manual centroid gate size. The tracker must be in a manual track mode in order to select manual gate size. Button is lit in AUTO gate size mode.
Gate Size, Az., El. toggles	Two spring-loaded toggle switches which increase or decrease the gate size when in manual gate size mode. Push the switch up to

Table 5-3 (cont.)

	increase the size and down to decrease.
Threshold, Auto	Lighted pushbutton which toggles between automatic and manual centroid threshold modes. Button is lit in AUTO mode.
Threshold, toggle	Toggle switch which increases or decreases the centroid threshold value. Push the button up to increase (brighter grey-level) the centroid threshold, down to decrease.
Contrast, Auto	Lighted pushbutton which toggles between automatic or manual centroid contrast. Button is lit in automatic contrast mode.
Contrast, Pos, Neg	Two lighted pushbuttons which indicate the selected contrast or can be pressed to manually select the contrast in the manual contrast mode.
<u>Miscellaneous</u>	
APD	Lighted pushbutton which toggles between aimpoint designation (APD) on and off. APD may be enabled before or during a track run. When APD is enabled and while tracking, the operator may reposition the tracked target in the video FOV by manipulating the rate stick. Button is lit when APD is enabled. APD is automatically disabled when track is exited and must be re-enabled each time it is desired.
Track Mode, Auto	Lighted pushbutton which toggles between automatic and manual track mode selection. In auto mode the tracker will automatically select between centroid and correlation track modes. Button is lit when in automatic mode.
Track Mode, Cent, Corr	Two lighted pushbutton switches which indicate which track mode is being selected in auto track mode, and can be pressed to select a particular manual track mode.
Track Valid LEDs	Two LEDs which indicate if either or both of the track gates have achieved a "TRACK VALID" state after track has been initiated.

Table 5-3 (cont.)

Display,  
Raw, Auto, Alternate

Three position toggle switch which selects which video is being displayed on the tracker instrumentation video monitor.  
In RAW the video is simply the raw digitized tracker input video.  
In AUTO the video is the raw video before track is initiated, and active track gate video during track.

In ALTERNATE mode, the display video is raw before track and the non-active or alternate gate's video during track.

Reset

Lighted pushbutton which performs a "soft" reset of the tracker microcomputer. This resets the tracker mode control to the following default conditions: correlation auto gate size, auto W1, centroid auto gate size, auto threshold, auto contrast, auto track mode, APD off, not tracking.

Rate Stick

Two axis rate stick with a pushbutton. The rate stick is used to control the gimbal line-of-sight before track, and can be used to position the track point (see APD button) during track. Pushbutton on top rate stick initiates or terminates a track run.

BIT

Run

Lighted pushbutton which initiates execution of the tracker automatic built-in-test (BIT). The button is lit during BIT execution and can be pressed again to terminate BIT.

Pass, Fail LEDs

Two LEDs which indicate the pass/fail results of a built-in-test (BIT) run. Both LEDs are on during BIT execution. After BIT has finished, only one will be illuminated to indicate that BIT either passed or failed. More detailed information on which circuit area failed can be had via the tracker RS-232C serial port.

## 6. LCTS Technical Performance

Section 6 describes the effort which was funded for the LCTS program. The total program included preparation of the terminals for the initial delivery to WPAFB, maintenance and engineering support of the terminals, and the automatic acquisition upgrade to the terminals.

### 6.1 Terminal Preparation

Prior to initial shipment of the lasercom terminals for the LCTS program, several modifications were made to the terminals to add performance monitors for experiment data recording, facilitate ease of testing, and to ensure the required gimbal and transceiver performance. An Instruction Manual for the LCTS terminals was prepared and delivered with the terminals. This document provides a description of the terminal hardware, performance and operation as well as a discussion of the interfaces.

To facilitate dynamic testing, gimbal wiring was reworked to reduce friction and increase azimuth travel, and both gimbals were rebalanced. Gimbal angular position displays on the front panel were calibrated. Hall-effect sensors were added to provide outputs indicating that gimbal stop has been reached. The rear panel was reworked to add a hinged panel for easy disconnection of the gimbal cable set from the rack electronics.

A digital format was mutually defined with the Air Force and an RS-232 digital output was added to the video tracker. The RS-232 output indicates tracker status and provides a measurement of line-of-sight tracking error.

Neutral density filters were procured and characterized by our optics laboratory for their transmission at 0.9  $\mu\text{m}$ . A mount was obtained which allows the neutral density filters to be changed without requiring removal of the lens from the gimbal. Additional background filters were cut and mounted so that filters were available for all four communication and tracking detectors.

An experiment was performed with the old lasers which suggested that they could support pulse rates of 19.2 Kpps (19.2 Kbps with all one's) at full power for (at least) minutes at a time. This requires operation at 0.2-percent duty cycle, which is twice the manufacturer's rating.

In the block diagram of the communication transmitter and receiver in Figure 5-5, the location of the transmit/receive performance monitors is shown. The performance monitors were added with the fundamental requirement not to degrade the performance in the process of measurement. To characterize the transmitted laser pulses, we provided a direct fiber optic monitor, rather than an indirect calibration of power against laser diode voltage as was originally planned. A fiber optic transmitter monitor allows calibrated reproduction of the pulsed optical waveform from the transmitting laser diode. The received optical waveform is characterized by the post-AGC amplifier pick-off together with an output indicating the value of gain in the AGC circuit. This avoided the necessity of building a second ultra-wide dynamic range or logarithmic amplifier chain, and still allowed calibration of receiver responsivity.

A potential problem was identified in our On-Off-Keyed (OOK) transmitter handling non-return-to-zero (NRZ) data waveforms from the HP 1645A data error analyzer. This is because the transmitted laser pulse is triggered from the leading edge of the data pulse, and the NRZ waveform only provides a leading edge on the initial data pulse for a string of logical one's. The solution was to perform a logical "and" operation between the data and the output clock from the HP 1645A. Since the clock pulses are shorter than the data pulses, this forces the data pulses to return to zero with the clock pulses, and provides a leading edge for each data pulse to trigger a laser pulse. This solution was implemented and worked well as verified by zero error counts on the HP 1645A data test set.

New Laser Diode Labs LDT-350 lasers and the performance monitors (for the received waveform and AGC voltage) were installed at the Santa Barbara Research Center. The transmitting, receiving, and tracking apertures were then realigned. A fiber optic monitor for the transmitted optical waveform was added to each terminal in El Segundo. The terminals were then tested for overall communication and tracking performance and deemed to be in good working order.

Two cables were fabricated which extend the separation of the gimballed transceiver from the main electronics rack of each terminal by approximately 30 feet. The cables allow exterior placement of the gimbals away from the electronics racks at both the Building 620 tower and remote site locations, and placement on an instrumented van for dynamic tracking tests.

## 6.2 Terminal Maintenance/Support

The two LCTS terminals were shipped and arrived at WPAFB on December 9, 1986. The LCTS program manager and an engineer arrived at WPAFB on December 10 to provide engineering support. A draft copy of the Instruction Manual was delivered. One engineer stayed at WPAFB through December 17.

Initial inspection of the terminals revealed shipping damage to a video tracker electronics card, which was returned to El Segundo for repair. A servo card was repaired on-base. Other than one terminal's tracker board, both terminals were functioning quite well in both audio communications and tracking. Preliminary testing with the HP 1645A verified successful digital data transmission, as well, including the modification made to allow transmission of NRZ data. The AGC voltage monitor was operating properly by noting the change in voltage when neutral density filters were added. The Hughes engineers also assisted AFWAL personnel in developing software to capture the digital tracking error signals output by the video tracker, as described in the following paragraphs. This verified operation of both the video tracker output and AFWAL recording software.

The tracking error in the video tracker can be monitored via digital signals from a RS-232 output from the tracker, as described in the LCTS Instruction Manual. AFWAL and Hughes personnel successfully debugged and operated a software program on the Zenith personal computer in order to capture the digital tracker data. The unit of measurement of tracking error provided in the RS-232 tracker output is in digital pixels, with a least significant bit of  $2^{-8}$  pixels.

The tracker digital pixel units can be converted into angular units with a scale factor determined by the area array physical dimensions and camera optics. The linear full-angle field of view of the camera ( $\theta$ ) is given by

$$\theta = 2 \tan^{-1}(d/2f) \quad (\text{radians})$$

where  $d$  is the linear dimension of the array and  $f$  is the focal length of the camera lens. For small angles,  $\theta \approx d/f$ . The Hitachi VKM98 camera in the LCTS terminals uses a HE98222A MOS photodiode area array with 384 x 485 pixels. The physical array size is in the standard 4:3 ratio (horizontal:vertical) of commercial TV, with dimensions of 8.8 x 6.6 mm. Together with a 250-mm focal length camera lens, the overall field of view of the camera is 2.0 x 1.5 degrees. The video tracker then samples the analog video from the camera to redefine the pixel resolution as 320 x 240 digitized pixels. Each square digital pixel thus has an angular subtense of 110  $\mu$ rads. The tracking error is output to  $2^{-8}$  pixel resolution, which corresponds to 0.43  $\mu$ rads angular resolution.

The video tracker board (which was damaged during shipping) was repaired at the Hughes El Segundo facility and checked out. The tracker board was then shipped back to WPAFB and reinstalled by AFWAL personnel. (The cards are in a card rack assembly which facilitates easy removal and replacement.) The repaired board successfully passed the tracker's built-in test (BIT) and was then working properly.

An existing calibrated solar cell which was to have aided calibration of the terminals was unfortunately no longer available. Hughes engineers identified two options - either rebuilding and calibrating another large area solar cell, or purchasing a Hamamatsu biplanar phototube. Both are large area detectors which can capture the entire transmitted beam. The solar cell has greater responsivity and dynamic range, but responds to average power. The biplanar phototube has poor responsivity but can respond to fast optical waveforms. The labor associated with rebuilding the solar cell from existing schematics (and recalibration) was estimated at three man-days (\$1.75-2.0K), and the parts were under \$100 and readily available. Cost and delivery schedule for the biplanar phototube were obtained. AFWAL personnel decided not to pursue these options for cost/contractual reasons.

A Hughes engineer traveled to WPAFB for field support from February 2-6. He installed a repaired video tracker board which then functioned properly without further adjustment. Thirty foot interchangeable extension cables were installed and tested on each terminal. These cables allow remote operation of the operator's console from the transceiver gimbals. Some circuit adjustments in terminal 2 were implemented in order to increase the stability of the servo elevation drift compensation. The optical fiber transmitter power pick-offs were modified to use 1000- $\mu$ m core fibers and connectors to increase the fraction of coupled monitor power, without significantly degrading the transmitted beamwidth. Both terminals were then fully operational.

After some discussion with AFWAL personnel, the video tracker states associated with when the tracker is "successfully tracking" was redefined. The tracker is defined to have four possible states: IDLE, INITIATE, MAINTENANCE, and COAST. After the operator has pressed the track initiate button on the joystick the tracker enters INITIATE mode. Each track gate (centroid, correlation) has a logical variable called TRACK VALID which is displayed via LEDs on the tracker control panel. The actual definition of TRACK VALID varies, however, depending on track mode and the state of mode controls such as auto track mode, auto gate size, etc. When the type of track gate is manually selected, for example centroid tracking (which is appropriate for laser spot tracking), the tracker moves to MAINTENANCE state upon achieving TRACK VALID.

For manual gate selection, "successful tracking" was initially associated with the tracker MAINTENANCE state. However, after field testing, the output describing whether successful tracking has occurred was better represented by the TRACK VALID logical variable, and this was changed during the automatic acquisition upgrade period.

AFWAL personnel inquired regarding the DMT coast mode option. Coast Mode can be enabled in the tracker by pressing the three centroid contrast AUTO, POS, and NEG buttons simultaneously. Since the coast detection algorithms are meant for a cluttered environment and can sometimes cause the tracker to coast unnecessarily, we made the default mode to be such that coasting is disabled. Once enabled by pressing the three buttons, it will stay enabled until the RESET button is pressed or power is removed. A simple test to determine if coast is enabled is to initiate track on a stationary object and then obscure the camera lens with your hand. The track gate symbols should flash to indicate that the tracker is coasting.

A Hughes engineer traveled to WPAFB for field support from March 10-11. He was specifically attempting to correct a servo instability problem with one terminal which was previously fixed during a February trip, but had recurred. He checked the servo ground and found it was solid. He then noticed that the  $\pm 12$  V power supplies were fluctuating in voltage. First, he tried to stabilize the voltage by adding capacitors, but without success. Next, he found that when the torquer motors were running (high current situation) there was a significant voltage drop in the terminal wiring. He then bypassed some of the wiring with new wires for servo ground and power, which seemed to clear up the problem.

A Hughes engineer traveled to WPAFB (Dayton) for engineering field support March 31-April 2. One of the terminals had a recurrence of servo instability which was then attributed to power supply and ground loop problems.

The terminals were shipped back to El Segundo for the automatic acquisition upgrades. The first terminal, which was shipped earlier, was entirely reworked in the area of power supplies and grounding. This eliminated the servo instability problem on this terminal and any common mode voltages present on parameter measurement outputs. Although there were no servo instability problems with terminal #2, the power supply/grounding was similar to terminal #1 and was also completely reworked. Low pass filters were added to the video sync strippers in both video trackers. These improvements, together with the previous reworking of the video tracker board grounding wires, greatly enhanced the stability and reliability of the LCTS terminals as reported by AFWAL personnel during the second phase of testing.

The angle position readouts on both terminals were modified to increase stability. A voltage regulator was added to prevent fluctuations in power supply voltage from influencing the angle readout scale factor. BNC connectors were added to the back of each terminal to increase operator convenience. An additional angular position output was provided to the tracker microcomputer in order to close a position loop for acquisition scanning control.

All of the video tracker cards in both terminals were reworked to increase field reliability. All of the problems to that date had involved the grounding wires on the cards, which were rewired to include redundancy.

An intermittent pulse dropout problem reported by AFWAL personnel was caused by a faulty connector on modem box #1. After repair of the connector, the laser pulse outputs were stable and zero errors were counted with the HP 1645A data system. The modem box capability for handling NRZ data (multiple ones in a row), obtained by "anding" the clock and data, also worked with the HP1645A with zero errors. The same tests were performed on modem box #2 which also counted zero errors. (However, modem box #2 had a resistor which appeared discolored and was replaced.)

During the week of May 11, AFWAL personnel observed the elimination of the servo instability of terminal #2 and the acquisition spiral scan plotted on a personal computer display in real time. We demonstrated our troubleshooting of the modem box, which resulted in replacing of a connector pin, and the data testing which then counted zero errors.

We had several delays during the automatic acquisition upgrade due to personnel losses and changes.

After the power supplies were reworked, the 30-foot cables introduced some additional audio and video noise which was reduced to manageable levels. The video noise comes from the laser pulses (100 nsec) traveling over twisted pair wires. It was impossible to keep the noise completely out of the camera even using an external battery and external shielded video cables. It appears that the transmit and receive wires which run through the gimbal will have to be replaced by shielded twisted pairs to eliminate the video noise, which requires rewiring the gimbal. For now, the procedure to manually set the threshold in section 6.3.2 eliminates the effect of the video noise on acquisition and tracking.

The capacitance of the 30-foot cables also contributes some audio noise which was minimized by capacitive decoupling in the modem boxes and by tuning the 6-kHz oscillators for voice mode to be more exactly matched. This reduced the noise to an acceptable level for the long cables. However, during this testing some electronic parts failed in one of the gimbal's transmit electronics. This required replacing a transformer and two FETs, but the laser was undamaged. This was repaired and the gimbal was shipped separately to WPAFB two days after the other hardware.

### 6.3 Automatic Acquisition Upgrade

Hughes personnel demonstrated highly successful automatic acquisition (scan and transition to automatic tracking) with the LCTS lasercom terminals to AFWAL engineers during the July 13-16 visit to El Segundo. We then demonstrated terminal-to-terminal automatic acquisitions over short ranges that averaged over 80-percent success. Subsequent to this visit, we refined the algorithm further, and this has eliminated the source of the few unsuccessful scans we encountered during short-range testing. We understand that Avionics lab personnel have conducted highly successful automatic acquisition and subsequent communications/tracking over the 5-mile test range between the Bldg. 620 tower and the remote test facility at Trebein.

#### 6.3.1 Acquisition Description

The LCTS lasercom terminals include a microcomputer-based video tracker which provides the scan management and control for automatic acquisition. The microprocessor is capable of generating angular tracking commands to the servo electronics, and is under-utilized prior to automatic tracking. Thus, we were able to add the acquisition function mostly in tracker firmware, with the addition of a buffered potentiometer measurement of gimbal angular position in order to close a first-order position loop with the tracker.

The center of the acquisition scan is designated by operator joystick control, and the scan is referenced to an angular position loop based on the gimbal potentiometer outputs. One terminal is designated as the acquisition transmitter and the other as acquisition receiver. (This is selectable on each terminal.) Each of the terminals performs a spiral scan for acquisition, with the transmitter scanning the entire scan field of regard (FOR) in the time it takes for the receiver to scan one acquisition cell. (A spiral scan is superior to a raster scan since it begins the scan at the most likely position of the target, enhancing the possibility of finding the target early in the scan pattern.) The acquisition time is dominated by the receiver scan time for this approach (which results from current hardware constraints). In section 7.1 a next-generation automatic-acquisition system is outlined which could eliminate the receiver scan, dramatically reducing the acquisition times.

An acquisition cell is defined by the terminal beamwidth or field of view (FOV), as appropriate for the acquisition transmitter or receiver. For the acquisition transmitter, the number of acquisition cells is defined as the total scan FOR divided by the transmitter beamwidth. The present transmitting beamwidth is  $0.5^\circ$ , which can be treated as  $0.4^\circ$  to allow for beam overlap. In order to facilitate faster acquisition times, the number of acquisition cells for the acquisition receiver are given by the scan FOR divided by the video tracker FOV. Since the video tracker FOV is  $2.0^\circ \times 1.5^\circ$ , the larger FOV gives fewer acquisition cells which results in a shorter acquisition time. The acquisition receiver cell size is taken as  $1.4^\circ$  to allow for overlap. The spiral scan is implemented with constant scan velocity so that the effective dwell time per acquisition cell is constant. For both acquisition transmitter and receiver the dwell time per acquisition cell is 1/30 sec, which is one frame time for the video tracker.

The acquisition field of regard (FOR) is selectable between 3, 6, 9, and 12 degrees. The worst-case acquisition times are given by the receiver scan period plus one transmitter scan period plus one transmitter slow scan period. These worst case times are given by 1.1, 3.1, 10.0, and 27.3 minutes for 3, 6, 9, and 12 degrees, respectively (assuming the receiver does not miss the transmitter). Because the operator designates the center of the scan by joystick control, and by using a spiral scan, the expected value of the acquisition times should be much less than the above worst-case values.

### 6.3.2 Acquisition Procedure

The video tracker control panel on the LCTS lasercom terminals has been modified so that existing switches are reprogrammed for acquisition mode. A comparison of the regular video tracker control panel in Figure 5-11 with the tracker control panel in acquisition mode (Figure 5-12) shows the CONTRAST buttons have been reprogrammed to handle the acquisition operator controls (relabelled SCAN).

Upon initial power-up, or after pressing RESET, the tracker is in regular mode. In regular mode, pressing the joystick causes the tracker to attempt to initiate track. To select acquisition mode, press the ACQ button and the tracker is now in acquisition mode. In acquisition mode, pressing the joystick causes the tracker to initiate the acquisition scan sequence centered at the current angular location.

Upon initial power-up, or if lighting conditions have changed significantly, a background threshold scan should be performed. This scan sets the tracker gain and offset to exclude the background levels observed during the scan. The background scan must be performed with the other terminal transmitter turned off. To initiate the background scan, press RESET, then hold down the TX button while pressing ACQ. The background scan will then commence over 12 degrees and lasts about 66 seconds. Then the threshold should be manually adjusted with the other terminal transmitter turned on. The threshold should be raised until the laser spot just disappears, and then backed off until the laser spot just returns. This establishes maximum thresholdability of the other transmitter. (Note that the next generation acquisition scheme, described in section 7.1, would essentially eliminate the need for manual threshold adjustment.)

The terminal can be designated as acquisition transmitter or receiver by the TX button; when lit the terminal is a transmitter; pressing it again will switch to receiver (with the button unlit). The scan field of regard (FOR) is selected with the FOR button; repeated pressing cycles between 3, 6, 9, and 12 degrees as indicated by the LED displays.

Once the acquisition buttons have been properly selected, pressing the joystick button initiates the acquisition sequence. For best results, the sequence should be initiated simultaneously at both terminals. (If they are not, the receiver may require two scans in order to acquire.) The operator then need only wait until both terminals have entered the regular centroid tracking mode.

### 6.3.3 Acquisition Logic

In order to implement the automatic acquisition algorithm some changes were required to the initially simple acquisition logic flowcharts. The major effect was to the logic for the acquisition transmitter, because the rapid transmitter scan rate caused a stationary distant laser spot to be blurred into 10-20 pixels on the video array. This resulted in a diluted video SNR which was not consistent with our requirement that the acquisition range performance should not be significantly less than the tracking range performance. Therefore we changed the logic so that the transmitter fast scan is stopped upon receiving a communication threshold crossing only (instead of both comm and video), and a second slow 3-degree spiral scan is initiated at the point of the comm threshold crossing. The center of the slow scan is determined by angle feedback from the gimbal potentiometers, and the scan rate is ten times slower such that the laser spot is essentially unblurred. The slow scan is 3 degrees for all acquisition fields-of-regard because it is sized to account for position loop inaccuracy, timing errors and gimbal inertia.

The final acquisition logic flowcharts are given in Figures 6-1 and 6-2 for the acquisition receiver and transmitter, respectively.

### 6.3.4 Acquisition Implementation

The bulk of the automatic acquisition implementation was accomplished in software using the microcomputer in the DMT video tracker. However, feedback from the gimbal angular position is required as an (A/D) input to the tracker in order to generate inertial scans with a position loop. A technical difficulty arose with the potentiometers which measure the gimbal angular position which was solved by replacing the mechanical interfaces between the potentiometers and the gimbal. This enables closing a position loop to command the gimbal during the acquisition scan to 0.1 degree accuracy (necessary to ensure beam overlap).

The acquisition scan subsystem requires a position loop to ensure that the scan is implemented with sufficient accuracy to ensure beam overlap ( $< 0.1^\circ$ ). The position loop feeds back the actual gimbal angular position to the scan microcomputer, so that the computer can assess how faithfully the gimbal has followed the angular commands. We found that the gimbal was initially not accurately following the scan commands with the position loop closed, and testing indicated that the potentiometers in the gimbal were exhibiting a hysteresis effect which limited the angular resolution. Inspection of the potentiometers revealed that the mechanical coupling of the pots to the gimbal was substandard on both gimbals. We placed a special rush order to obtain the proper helical mechanical couplings (\$50 each) and installed them on both gimbals. We were then able to obtain the necessary 0.1 degree accuracy.

Maximum angular rate and acceleration were measured for gimbal #2 in order to determine the maximum scan rates the gimbal would support for acquisition. By applying step rate commands with a waveform generator, the maximum rate was found to be about  $73^\circ/\text{sec}$  in azimuth ( $110^\circ/\text{sec}$  in elevation), and maximum acceleration was about  $224^\circ/\text{sec}^2$  (all saturated values). We have decided to derate the maximum acceleration to a value of  $150^\circ/\text{sec}^2$  for the acquisition scan (to avoid saturation).

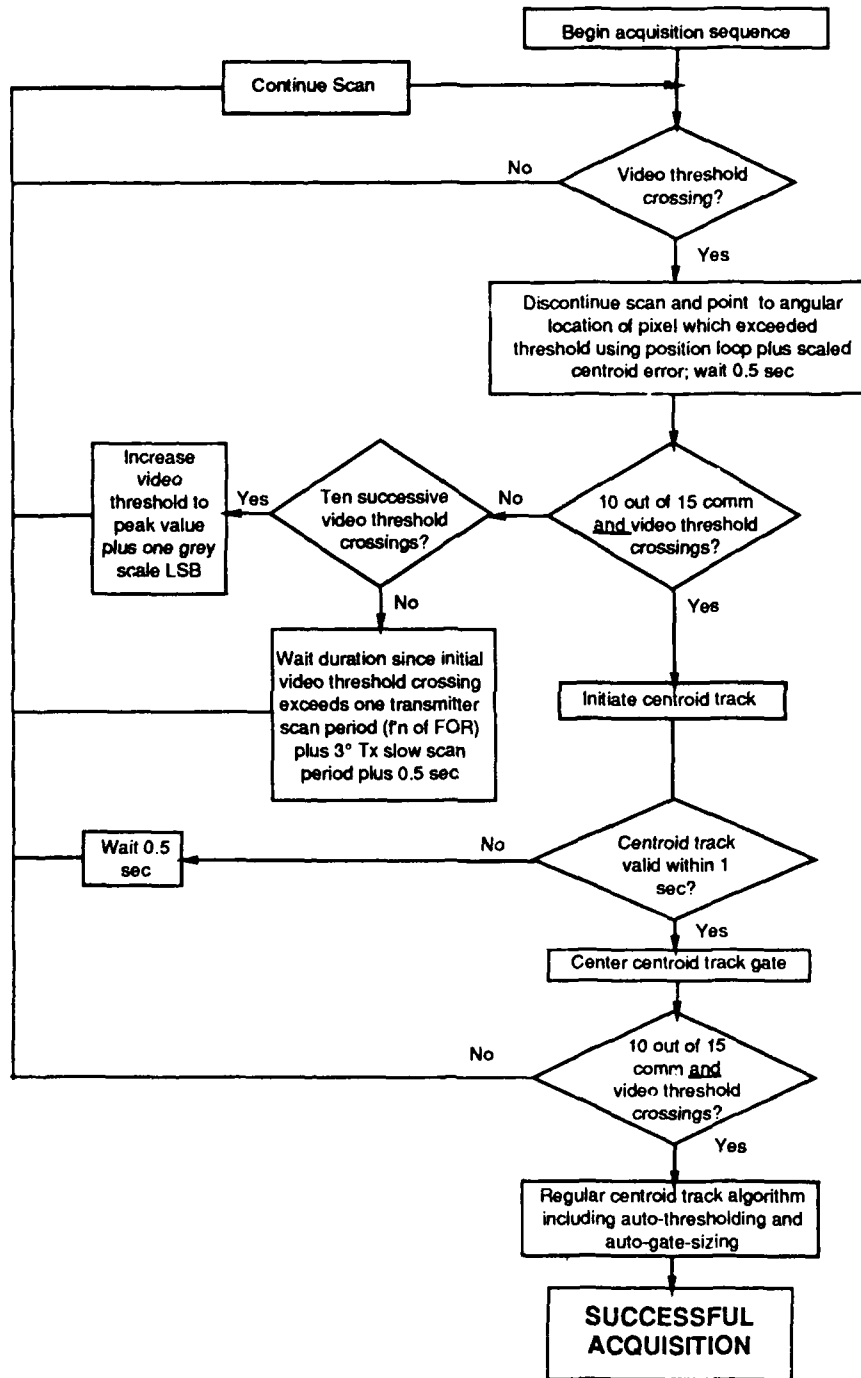


FIGURE 6-1. ACQUISITION LOGIC FLOWCHART - RECEIVER

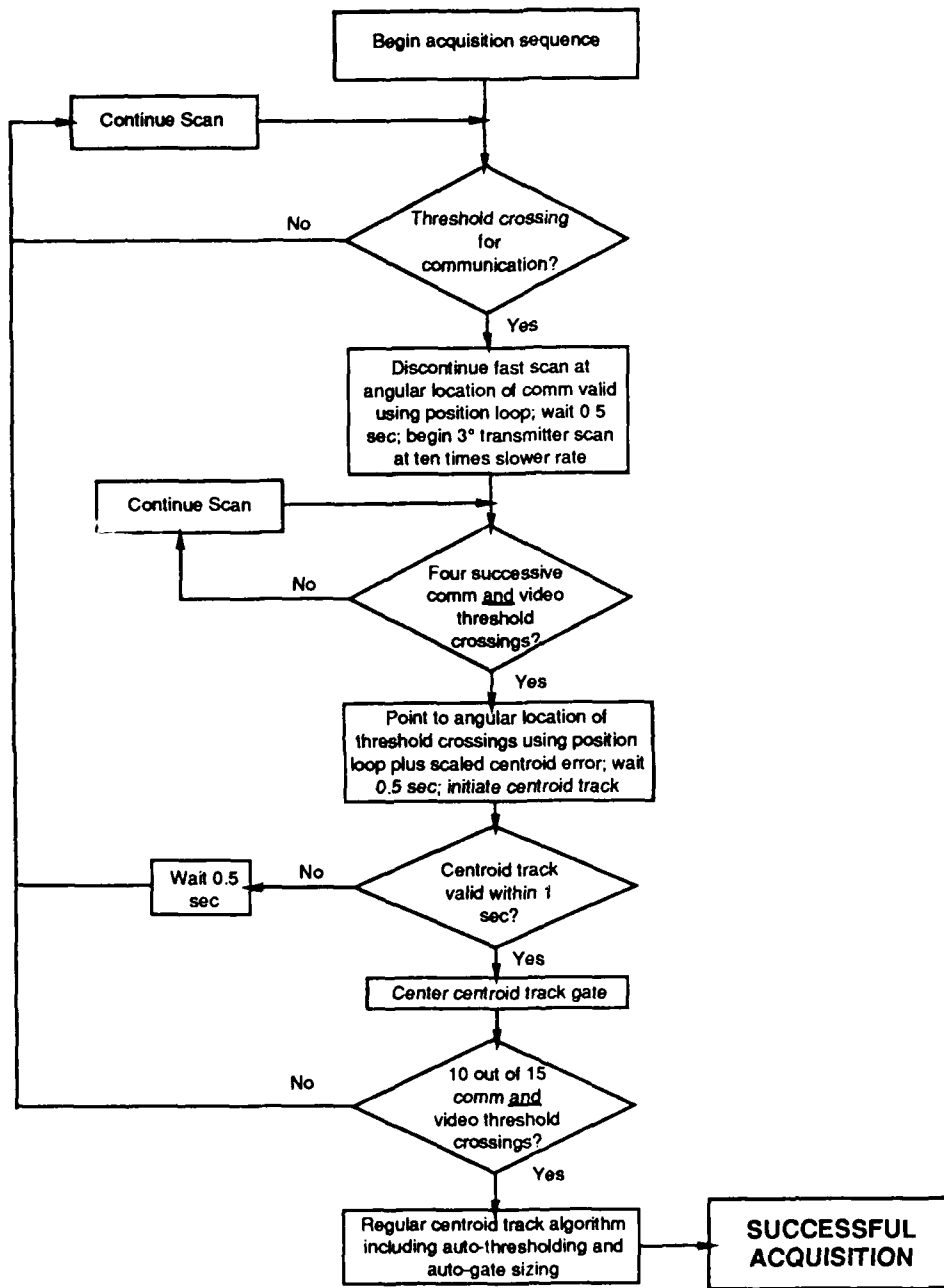


FIGURE 6-2. ACQUISITION LOGIC FLOWCHART - TRANSMITTER

Figure 6-3 shows a plot of the angular commands to the gimbal for the transmitter spiral scans of 3, 6, 9, and 12 degrees, which include the flyback to center. The amount of time required for each of the transmitter scans is noted next to the plot. (Recall the acquisition receiver covers 1.4 degrees during one complete transmitter scan.) Note the excellent fidelity of the scan commands.

Figure 6-4 shows a plot of the 12-degree transmitter scan actual gimbal motion before the potentiometers were upgraded. Note the "square" character of the supposedly circular scan. Although the width between the scan lines is fairly constant, the hysteresis has a more drastic effect on the ability to accurately fly back to center. Figure 6-5 shows the same 12-degree transmitter scan after the potentiometers were upgraded. Note the greatly improved scan fidelity. (There is still some jitter on the plot due to the gimbal inability to exactly follow the commands and the finite bandwidth of the type I position loop.) Figure 6-6 shows the 12-degree receiver scan and, although the scale factor on the plot is half that of Figure 6-5, the jitter is less noticeable for the slower receiver scan due to its slower rates.

During acquisition testing at close ranges we found that the communication field of view (FOV) could be much larger than the  $0.6^\circ$  as calculated by the physical size of the detector active area (0.1 inch) divided by the lens focal length (250 mm). The comm FOV could actually be larger than the track gate at higher signal levels which disturbed the algorithm. This problem was solved by machining spatial apertures (0.55-inch diameter) which were placed in the plane of the detector. This limits the comm FOV to about 0.8-1.0 degrees even for high signals.

## 7.0 LCTS Technical Discussion

### 7.1 Next Generation Automatic Acquisition System

A next generation automatic acquisition system has the potential to drastically reduce the required acquisition times compared to the current auto-acquisition scheme. For example, the 12 degree worst-case times could be reduced from 27 minutes to under 2 minutes. This could not be implemented within the current program due to hardware limitations of the camera FOV and the current capability of the video tracker. The next generation acquisition system requires a 6:1 zoom lens on each camera and utilizes the most recent Hughes video tracker innovations - difference video and complementary tracking.

The current acquisition scheme defines an acquisition transmitter with a  $0.5^\circ$  (taken as  $0.4^\circ$  for overlap) beamwidth and an acquisition receiver with a field of view (FOV) of  $2.0^\circ \times 1.5^\circ$  (taken as  $1.4^\circ$  for overlap). The acquisition transmitter scans the entire acquisition field of regard (FOR) during the time the acquisition receiver dwells on one acquisition cell. Thus the transmitter scans the FOR many times before the receiver completes one FOR scan. The worst-case acquisition time is given by one transmitter fast scan period plus one transmitter slow scan period plus one receiver scan period, but the acquisition receiver scan dominates the required acquisition time.

The worst-case acquisition times could be dramatically reduced with the combination of hardware and software improvements to the current LCTS hardware. By incorporating a zoom lens for the video camera array and incorporating difference video into the DMT video tracker, the

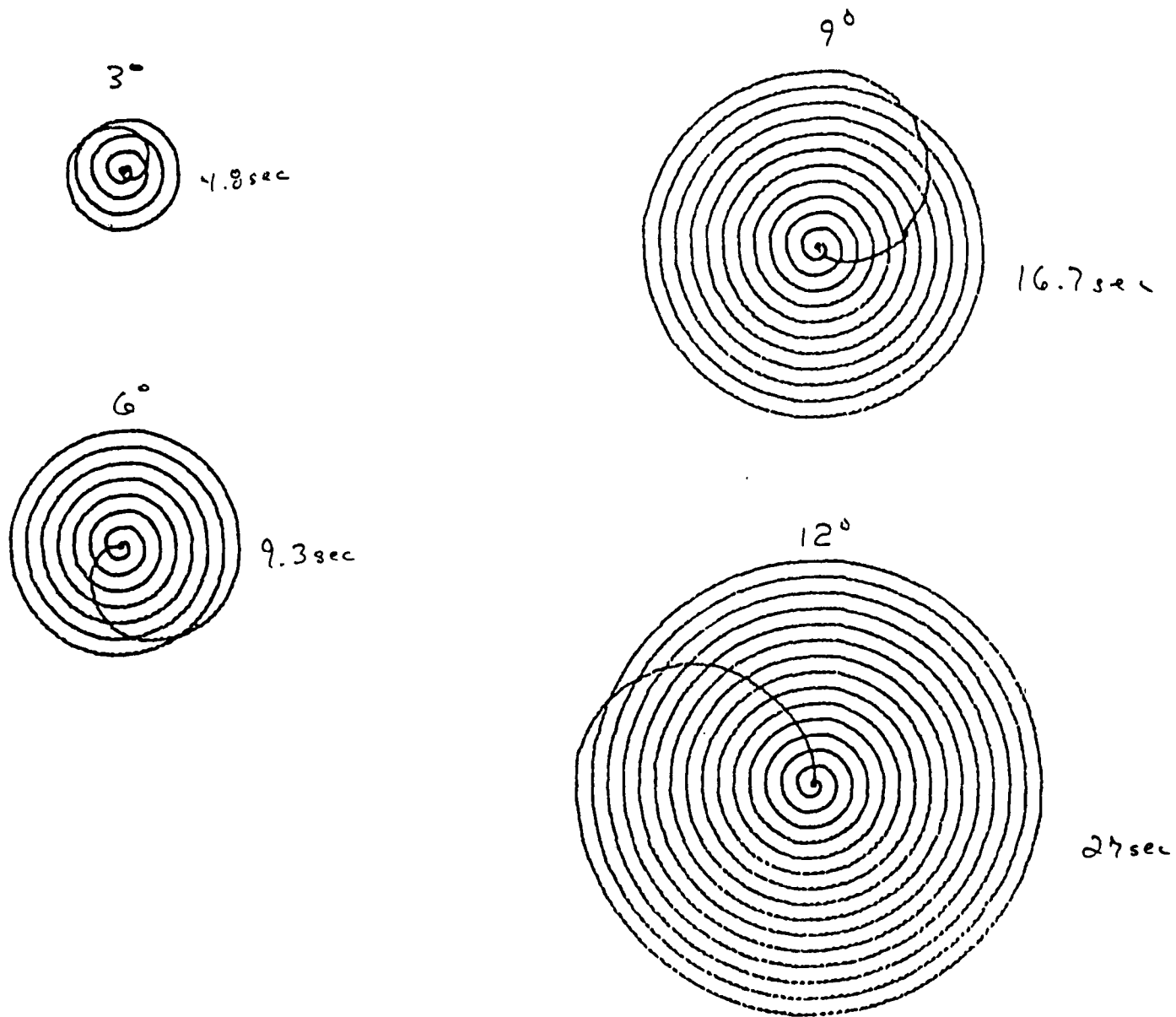


Figure 6-3. Plot of Angular Commands for Spiral Scans of 3, 6, 9, and 12 Degrees

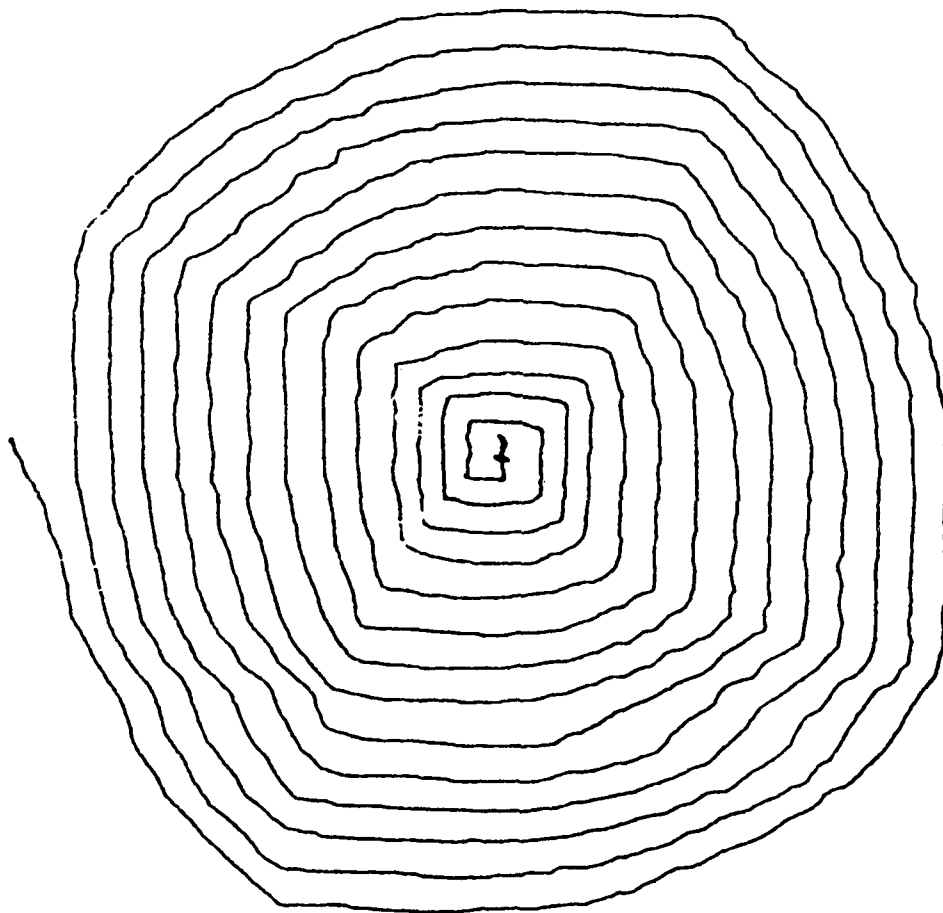


Figure 6-4. Gimbal Motion for 12-Degree Transmitter Spiral Scan  
(Before Potentiometer Upgrade)

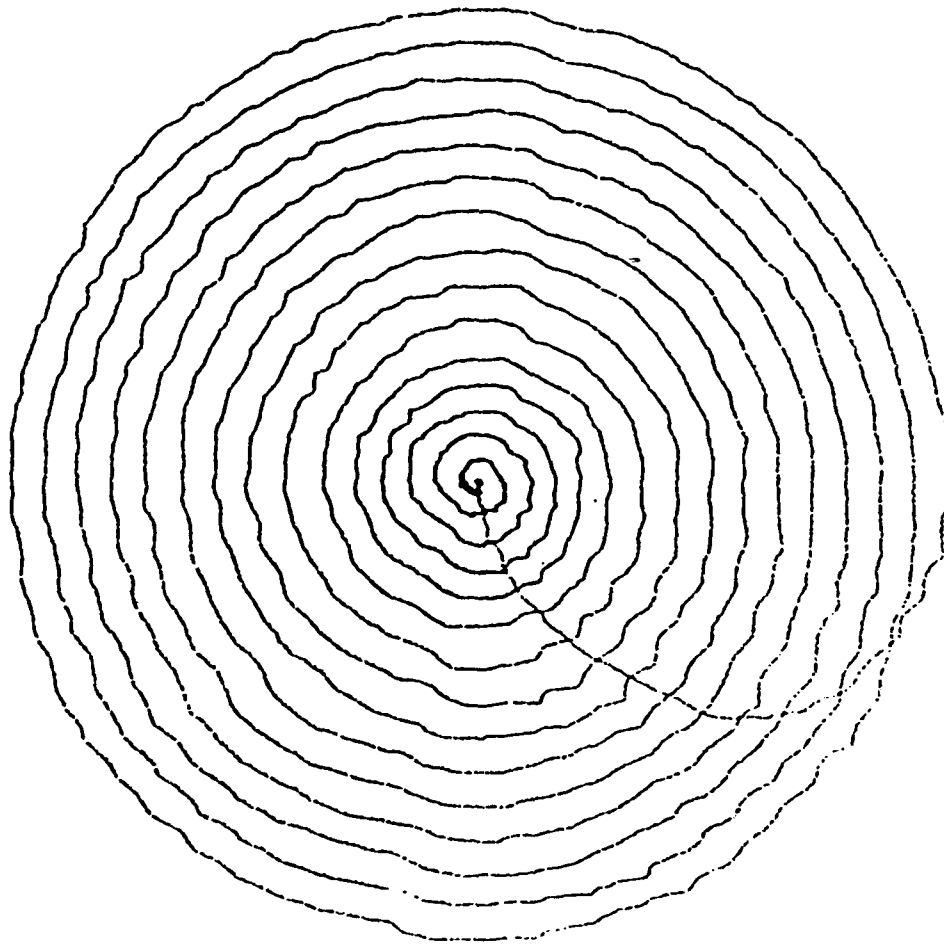


Figure 6-5. Gimbal Motion for 12-Degree Transmitter Spiral Scan  
(After Potentiometer Upgrade)

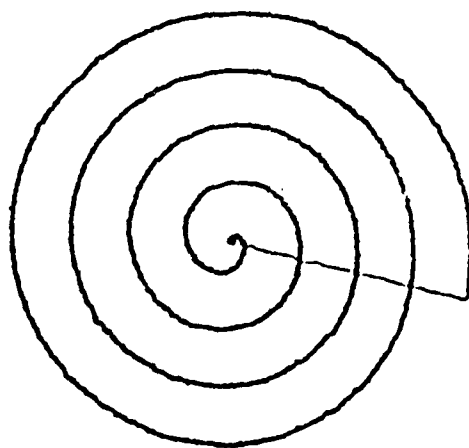


Figure 6-6. Gimbal Motion for 12-Degree Receiver Spiral Scan  
(After Potentiometer Upgrade)

acquisition receiver could stare into the entire acquisition FOR. By staring into the acquisition FOR the array difference video allows the acquisition uncertainty to be reduced by a factor of 400 within one video frame of being illuminated by the distant terminal. This eliminates the need for an acquisition receiver scan and reduces the worst-case acquisition time to two transmitter fast scan periods plus one transmitter slow scan period. For example, for a 12-degree acquisition FOR this reduces the acquisition time from 27 minutes to under 2 minutes. (The factor of acquisition time reduction for this improved scheme is proportional to the square of the acquisition FOR.) An acquisition scheme with a 12-degree FOR and under 2 minutes acquisition time is quite attractive for an operational system.

The utilization of difference video in the video tracker processing exploits the addition of a 6:1 or 8:1 zoom lens to the video camera. Difference video subtracts the current video frame from the previous frame and then processes the difference frame. This reduces the effective frame rate by a factor of two, but removes the DC noise sources due to array fixed pattern noise and fixed optical backgrounds. The array increases the array sensitivity substantially as it is then limited by random shot noise and thermal noise. The acquisition receiver must be inertially stabilized, as with the current gyro-stabilized gimbals, for the scene to appear "fixed" so that unchanging detector and optical background signals are removed. This frees the distant laser terminal to only have to be the brightest "new" target, but not necessarily brighter than the unchanging "old" sources.

The addition of a zoom lens to the current gimballed system would require the addition of stronger torquer motors and rebalancing the gimbals, in addition to reworking the mechanical interfaces for the camera and electrical interfaces to control the zoom. The addition of a zoom lens with difference video not only improves the sensitivity, as just described, but also eases the problem of manual threshold adjustment. Since empirical thresholds are applied in difference video they are far more robust. Even long term operator adjustment of thresholds based on optical background might be eliminated with this approach.

## 7.2 Comparison of Video and Quadrant Tracking

This program did not include any analytical comparisons of quadrant and video tracking. The first issue is the sensitivity of the sensors, which could include intensified CCD or ordinary CCD array sensors, and avalanche photodiode (APD) or PIN quadrant trackers. Intensified CCD and APD quadrant detectors have the best sensitivity, but the intensified CCD is bulky, uses high voltage, and is difficult to place on-gimbal. However, for terrestrial aircraft laser communications during bright sky conditions the background radiation is significant and may eliminate much of the sensitivity advantage of a quadrant APD over a standard CCD array.

Each of the quadrant and array tracking schemes are capable of tracking to much less than 1/10 of the receiver optical blur (for high SNR). The array, with typically 400 x 500 pixels, can have a much higher instantaneous total field of view than a quadrant detector of similar tracking accuracy. This allows the array to serve as both the acquisition and tracking detectors, so long as the array frame rate is compatible with the servo update rate as with an inertially stabilized gimbal (such as used on the LCTS terminals). A quadrant tracker system invariably must add a separate quadrant subsystem for the acquisition function.

Therefore, the array may be a better overall choice than a quadrant detector if the aircraft lasercom missions require bright sky system performance and the design includes either an inertially stabilized gimbal or a special high frame rate array.

## Appendix A. Spiral Scan Implementation

### 1. Introduction

A spiral scan has advantages relative to a raster scan for laser communication acquisition because the spiral begins at the most likely location of the distant receiver, reducing the average acquisition time. For the LCTS program, we have implemented in software the scan commands to generate a constant dwell time spiral scan with selectable fields of regard of 3, 6, 9, and 12 degrees. Numeric solutions of the spiral scan equations are computed at tracker power-up and stored in look-up tables. These tables are interpolated in real time by the microcomputer to provide the selected field of regard. A slight modification was made to the scan commands to reduce the gimbal acceleration requirement at the beginning of the scan, which resulted in negligible effect on acquisition time.

### Spiral Scan

The basic equation of a spiral scan for laser communication is given by

$$R = \frac{D}{2\pi} \theta$$

D = Transmit beamwidth or receiver FOV (deg)

R = Scan Radius (deg)

$\theta$  = Scan Angle (rad)

To verify the equation, it can be seen that the scan radius changes by one transmit beamwidth (or receiver FOV) for each revolution of the scan ( $2\pi$  change in  $\theta$ ). In order to ensure that each acquisition cell receives a full video frame worth of transmitter illumination, the spiral scan must be implemented with constant tangential scan velocity. For a constant scan velocity ( $K_S$  in deg/sec), the magnitude of the resultant tangential and radial velocity components is set equal to  $K_S$ ,

$$\sqrt{(\dot{R})^2 + (R\dot{\theta})^2} = K_S$$

but

$$\dot{R} = \frac{D}{2\pi} \dot{\theta}$$

and

$$R\dot{\theta} = \frac{D}{2\pi} \theta \dot{\theta}$$

Thus

$$\frac{D}{2\pi} \dot{\theta} \sqrt{1 + \theta^2} = K_S$$

And

$$t = \frac{D}{2\pi K_s} \int_{\theta_1}^{\theta_2} \sqrt{1 + \theta^2} d\theta$$

Thus:

$$t = K_N \left[ \theta_2 \sqrt{1 + \theta_2^2} + \ln(\theta_2 + \sqrt{1 + \theta_2^2}) - \theta_1 \sqrt{1 + \theta_1^2} - \ln(\theta_1 + \sqrt{1 + \theta_1^2}) \right]$$

Where

$$K_N = \frac{D}{4\pi K_S}$$

### Transmitter

Due to the fact that the position loop bandwidth is limited to 1 to 1.5 Hz because of limit cycling induced by the gimbal acceleration limit (150-200 deg/sec<sup>2</sup>), it is necessary to slow the scan down at the beginning so that a 1-1.5 Hz position loop can follow the scan command.

If a maximum rate of 1 rev/sec is used,  $\dot{\theta} = 2\pi$  rad/sec. Using a scan rate ( $K_S$ ) of 0.4° in 1/30 seconds yields a scan rate of 12°/sec. For the perfect spiral  $\dot{\theta}$  decreases as  $\theta$  increases. Solving for  $\theta$ , where the perfect spiral is given by  $\dot{\theta} = 2\pi$  rad/sec, yields:

$$\frac{D}{2\pi} \dot{\theta} \sqrt{1 + \theta^2} = K_s \text{ or } \sqrt{1 + \theta^2} = \frac{K_s (2\pi)}{D \dot{\theta}}$$

$$\theta = \sqrt{\left(\frac{2\pi K_s}{D \dot{\theta}}\right)^2 - 1} = \sqrt{\left(\frac{12(2\pi)}{(.4)(2\pi)}\right)^2 - 1} = 29.9833$$

Since the scan points were computed every 0.1 sec  $\theta = \theta + \Delta\theta$  where  $\Delta\theta = 0.2\pi$ , it takes 47.72  $\Delta\theta$  increments to yield 29.9833 rad. Using 48 points the transition angle is 30.159289 rad (angle at which the scan becomes true constant dwell time spiral scan).

### Receiver

The receiver scan rate is set such that the receiver FOV (1.4°) is scanned in the time required for the transmitter to complete its scan plus retrace. For the receiver table, the transmitter scan periods used were

<u>Scan FOR</u>	<u>Period (sec)</u>	
3	2.5	
6	7.5	(Really 7)
9	15	(Really 14.5)
12	25	

Larger numbers were selected so that all the periods were multiples of 2.5 sec.

For the 2.5 second scan period

$$K_s = \frac{1.4}{2.5} = 0.56^\circ / \text{sec}$$

$$K_N = \frac{1.4}{4\pi(.56)} = \frac{0.625}{\pi}$$

The table was generated for scan points every 1 sec (2.5 sec scan period). Since the other scan periods were short scan periods, the desired scan patterns can be generated by scaling the time values associated with the points in the table.

## Appendix B Hughes Dual Mode Tracker (DMT) Description

### 1. AVT Functional Description

Both a proven silhouette centroid and a powerful matched filter (i.e., optimal weighting function) correlation algorithm employing a recursive reference (Hughes patent 4,133,004) are utilized for the basic tracking error computations

Figure B-1 is a simplified block diagram for the tracking processor. The four processing functions and the key input-output signals for the individual functions and the overall tracking processor are identified. These processing functions are described briefly in the following paragraphs.

### 2. Video Preprocessing Function

The video processor provides an accurate general purpose input video interface for the tracking processor. In addition to the basic video analog-to-digital conversion function, anti-aliasing filtering, video gain and offset actuation, gated video peak and valley detection, and configurable pixel averaging or pixel rate buffering functions are provided in the video preprocessor. Following analog offset and gain operations, the input video is encoded to 7 bits. Gated video peak and valley detection for automatic gain control is performed digitally. Thus, 7-bit encoding is utilized in order to generate a 6-bit output video and to provide an appropriate dynamic range for video peak and valley detection. Pixel averaging is provided in order to average intensity values for pixels in adjacent video lines. This function can also be configured for pixel rate buffering when the pixel data rate exceeds the 6-MHz limit imposed by particular hardwired processing functions. The output video from the preprocessor is encoded to 6 bits and is sent to both the correlation and centroid processing functions and is available at the instrumentation video output port. Automatic gain control (AGC) spatial gating commands along with video gain and offset commands which are derived from the video peak and valley data are generated by the microcomputer function.

### 3. Centroid Processing Function

The centroid processor contains the hardwired functions required to accurately perform the centroid track error processing function. A proven silhouette centroid algorithm is used. For positive (negative) contrast targets, the video above (below) threshold is converted to a fixed value, thus yielding binary video where all the video rejected by the threshold is zero. Target contrast and video threshold values are derived via processing video intensity histograms for the track and a surrounding border gate. Although the track video is binary, the threshold is defined with 6-bit resolution. Track gate size control is implemented by detecting and processing the location of thresholded video edges. Silhouette centroid processing is depicted in block diagram form in Figure B-2. As indicated, the binary video output from the comparator operation is effectively multiplied (a gating operation is actually used) by linear weighting functions,  $W_e$  and  $W_d$ , which are determined by track gate size and position information and are derived from pixel counters in the video line direction and line counters in the orthogonal direction. Thus, binary video-weighting function products and the number of pixels passing the threshold are accumulated over the track gate. These accumulated sums,  $E_e$ ,  $E_d$ , and  $I_o$ , are the raw error parameters and are sent to the microcomputer function after the track gate is scanned each field. The actual track errors are then computed at the video field rate in the microcomputer function.

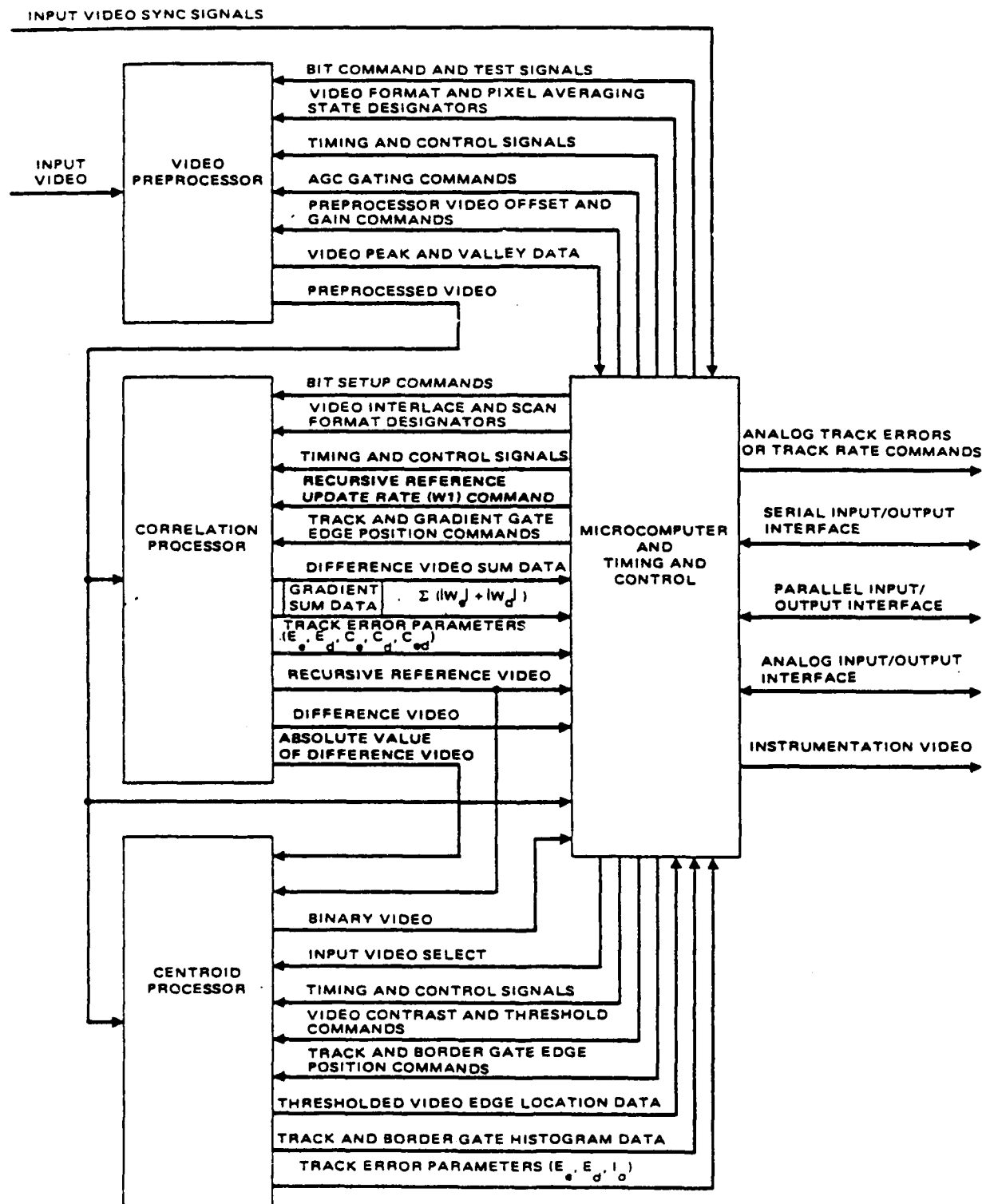


Figure B-1. Dual Mode Video Tracker Block Diagram

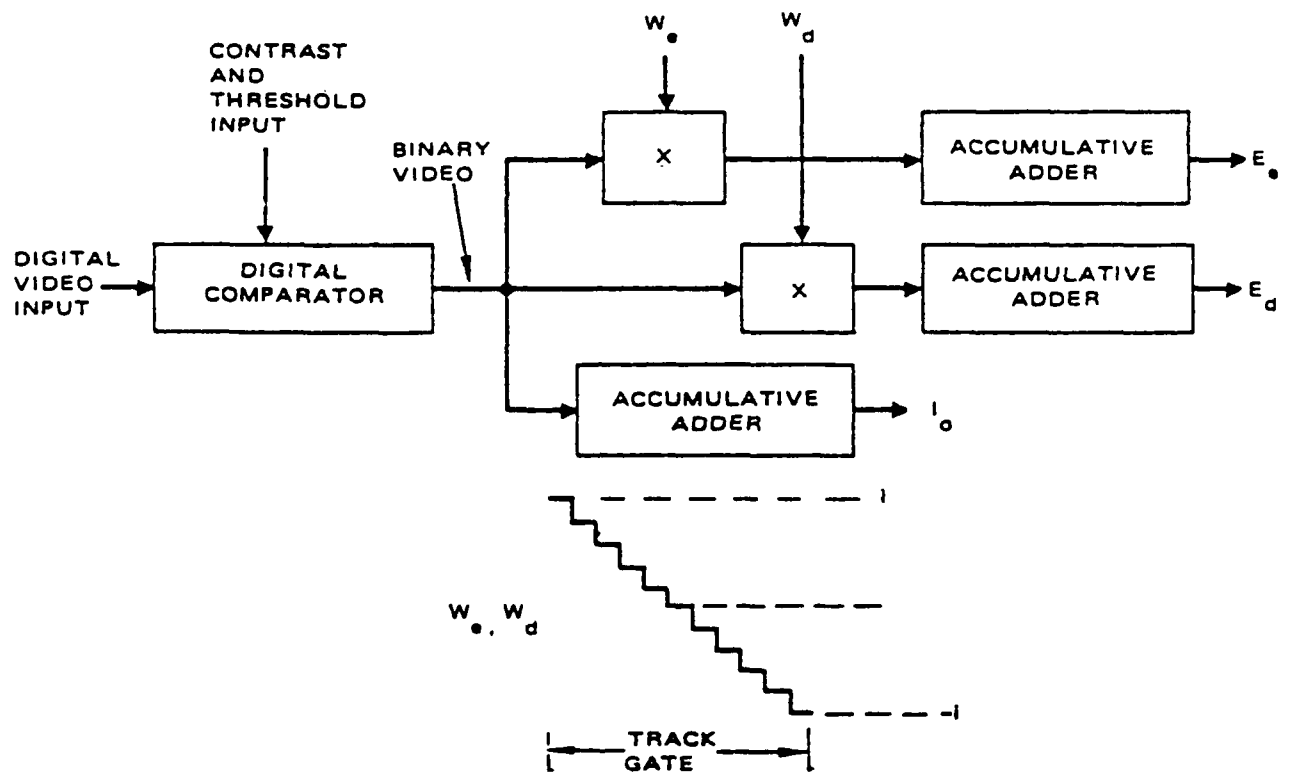


Figure B-2. Silhouette Centroid Processing Block Diagram

For a nonoverlapping 2:1 interlace video format, raw error parameter data from two successive fields is combined in the microcomputer computations as follows:

$$\Delta = \frac{E_E + E_O + K I_{OE}/2}{I_{OE} + I_{OO}}$$

where

- $\Delta$  = track error in pixels
- $E_E, E_O$  = sums of the products of the binary video and the centroid weighting functions of the even and odd fields, respectively
- $I_{OE}, I_{OO}$  = number of pixels passing the threshold value for the even and odd fields, respectively
- $K = 1$  in the interlace direction
- $K = 0$  in the scan direction

Ancillary hardwired centroid processing functions implemented in the centroid processor are the track and border gate histogram generators, binary video edge detectors, and video gating for the track and border gates. The border gate is concentric with the track gate, and the size relative to the track gate can be adjusted. Currently a 4-pixel border around the track gate is utilized.

#### 4. Correlation Processing Function

The correlation processor function provides several unique hardwired functions associated with implementation of the matched filter correlation algorithm and key ancillary processor control functions. Use of the matched filter algorithm make it possible to use a desirable "pipeline" processing technique. In this pipeline process, all of the stored reference scene and the current scene information within a track gate is utilized as the gate is scanned, thus yielding error signal data immediately after the track gate scan is complete, regardless of the size of the gate. This operation is unlike conventional correlation processors, which typically do a reference and a current scene search for the cross-correlation peak, and can be very time consuming, usually introducing time delays that significantly degrade the track loop performance potential and increase tracking following errors.

Another unique characteristic of the design is the use of a recursive reference-update technique. With this technique, old reference data has a lifetime associated with it, and new data is input in such a way that nothing is quickly added to the reference. Thus, the reference is updated smoothly so that changing target features (due to attitude or range changes and sensor roll about the line of sight) are accepted, but more rapidly changing information, such as noise clutter that passes through the scene or glints that pop up and move about on the target, are rejected. The use of the recursive reference is key to realizing robust correlation tracking performance in dynamic situations, and in clutter. Furthermore it can be shown that employing a recursive reference eliminates the undesirable random walk phenomenon that arises when the reference scene is repeatedly reloaded in other types of correlation processors.

The matched filter correlation processing technique is a unique and accurate means for locating the position of the peak of the cross-correlation function between the incoming scene and the reference scene. It is best viewed as the realization of a method for finding the location of the zero crossing of the cross-correlation function spatial derivative, which is mathematically equivalent to finding the peak of the scene-reference cross-correlation function. Employing a Taylor Series expansion, it can be shown that the zero crossing location can be computed by multiplying the pixel intensity differences between the incoming scene and the reference scene by weighting functions that are the horizontal and vertical spatial derivatives of the reference scene at

the location of the reference scene pixel being processed. The individual difference video-weighting function products for each pixel are generated as the incoming scene is scanned and are accumulated over the track gate of interest. Tracking errors are then obtained by appropriately scaling these accumulated products by the accumulated sums of the products and squares of the weighting functions. Weighting function generation and the appropriate pixel rate multiplications, along with the product accumulations, are executed in the hardwired correlation circuitry. This "pipeline" process is depicted in Figure B-3 for a simplified noninterlaced video format. In the figure, the horizontal and vertical weighting functions are designated  $W_{dij}$  and  $W_{eij}$ , respectively. The difference video is designated  $D_{ij}$  and is equal to  $V_{ij} - R_{ij}$ , where  $V_{ij}$  and  $R_{ij}$  are the incoming scene and the reference pixel intensity values, respectively. The remaining portion of the track error computation is executed in the microcomputer firmware once the track gate is scanned and the error parameter accumulated sum are available. This computation consists of scaling, a cross-coupling correction, and drift-removal processing. These computations are depicted in block diagram form in Figure B-4. Scaling consists of normalizing the raw track errors,  $E_e$  and  $E_d$ , by the appropriate squared weighting function sum. The cross-coupling correction operation utilizes the weighting function cross-product sum,  $C_{ed}$ , and removes error cross-coupling that otherwise occurs in many correlation processing algorithms when scene or target edges or intensity gradients are skewed relative to the horizontal and vertical axes.

Drift-removal processing compensates for the fact that the recursive reference is continuously updating with an update rate factor  $W_1$ . That is, as depicted in Figure B-5, the recursive correlation reference is generated by multiplying the input video pixel intensity values by a weighting factor,  $W_1$ , and adding it to the existing intensity value for the corresponding reference pixel after the reference value has been multiplied by  $1 - W_1$ . The "lifetime" of a particular scene in the reference is determined by the value of  $W_1$  (note  $W_1 \leq 1$ ). If  $W_1 = 1/60$ , for example, and the sensor field rate is 60 fields per second, the "lifetime" of a reference scene is one second. For drift removal processing, the past tracking errors are accumulated with a weighting factor of  $W_1$ , thus ensuring that the initial pointing reference is maintained even if dynamic following errors occur during reference update. Furthermore, with drift-removal processing dynamic following errors, many pixels in magnitude can exist without causing loss of lock (though in some circumstances the basic error processing algorithm provides error signals with limited dynamic range). The outputs of the drift removal processing are then scaled by the track video pixel sizes ( $\Delta_e, \Delta_d$ ) to yield the angular tracking errors ( $\delta_e, \delta_d$ ).

For interlaced video formats, recursive references are generated for each individual field. For a sensor with a 2:1 non-overlapping interlace the weighting functions in the interlace direction are generated using intensity values from adjacent pixels in the reference for the opposite field. The accumulated sums for the non-overlapping interlaced fields are then combined and utilized for a single track error computation that is updated each time new data is obtained from a field. With interlaced video formats, the  $W_1$  update rate factor indicated in the drift removal computation is the recursive reference update rate factor divided by the number of video fields per video frame.

Recursive update rate factors of 0, 1/64, 1/16, 1/8, 1/4, 1/2 and 1 are provided and are dynamically controlled via an algorithm implemented in the microcomputer firmware. An update rate factor of 1 which corresponds to a single frame is used to load a new reference. Zero is used to freeze the reference when transient clutter is detected, thus preventing clutter contamination. During a tracking engagement, a reference is loaded when tracking is initiated. The update rate factor is then decreased from 1/2 to smaller values in a programmed manner so as to optimize the noise filtering property of the recursive reference. Thereafter, the update rate factor is a function of the correlation track status and the frame-to-frame errors between the incoming scene and the reference. If the frame-to-frame error increases, the update rate factor is also increased, thus reducing the instantaneous misalignment between the incoming scene and the reference. When

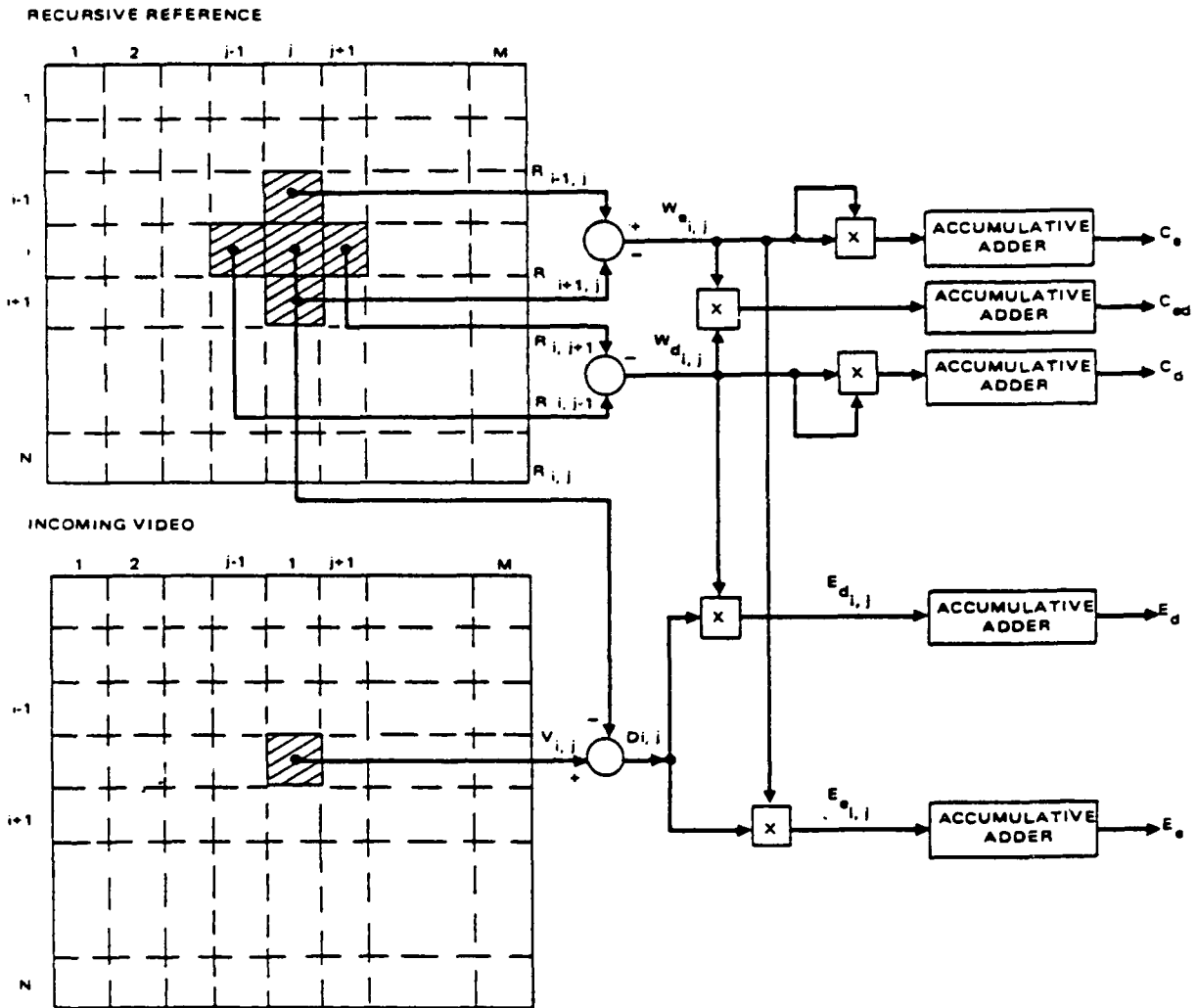


Figure B-3. Pipeline Processing for Matched Filter Correlation Processor

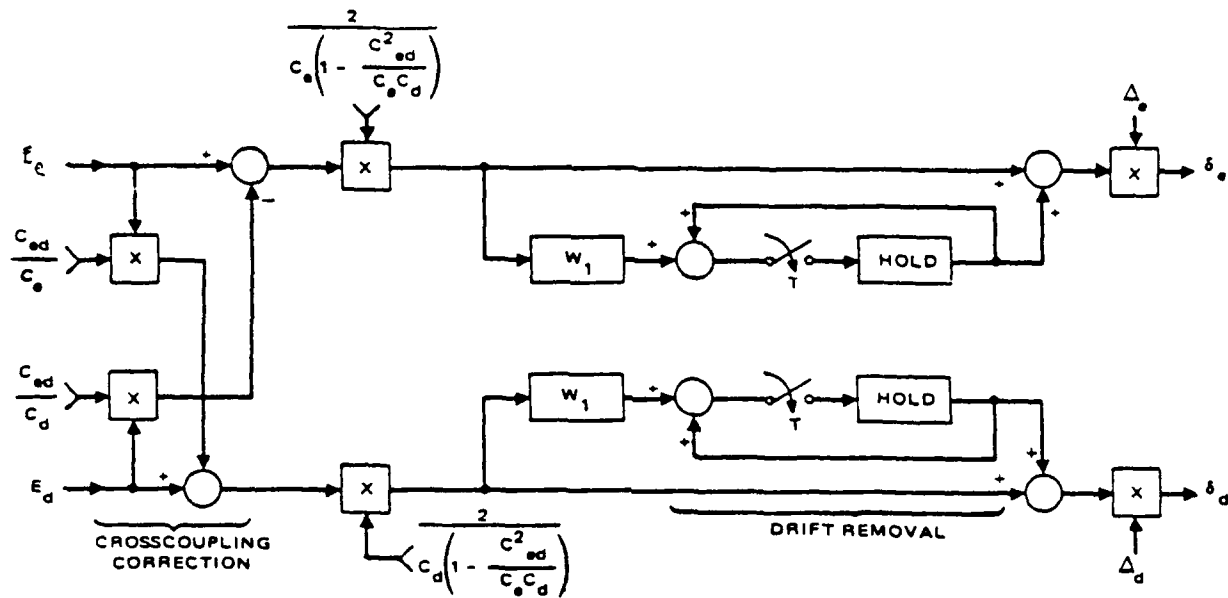


Figure B-4. Block Diagram of Correlation Error Computations Executed in Firmware

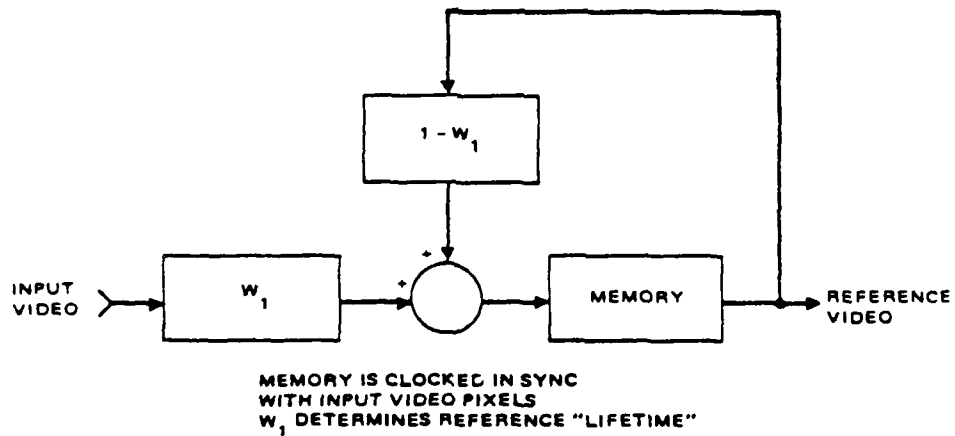


Figure B-5. Recursive Correlation Reference

clutter intrusion is detected, the reference is frozen. As indicated in the video preprocessor subsection, the input to the correlation processing function is 6-bit video. All 6 bits are used in the correlation error computations. Given 6-bit input video and a minimum recursive reference update rate factor of 1/64, 12 bits must be provided for each recursive reference pixel intensity value in order to properly accumulate intensity data in the reference. The 6 most significant bits are then used to generate the weighting functions and the difference video.

In addition to computations relating to the basic correlation tracking algorithm, several ancillary functions that are key to realizing fully automatic control are also implemented in the correlation processing function. These functions are scene gradient sum accumulation for track gate sizing, difference video sum accumulation for clutter detection, and video gating for both the track gate and an independent gradient gate.

Scene or target video gradients contain the information fundamental to correlation tracking. Thus, it is desirable to size the correlation gate so as to maximize this information content. In order to generate an appropriate measure of the desired information, a gradient function is generated for each reference pixel contained in the track gate. This gradient function is the sum of absolute values of the horizontal and vertical weighting functions for the pixel location of interest. This function is then accumulated over a gradient gate, and the gradient gate is dithered under microcomputer control so as to maximize the average value of this sum over the gradient gate. The gradient gate edge locations are then processed by the microcomputer to generate the desired track gate edge locations.

Under normal tracking conditions, the sum of the difference video over the track gate is small. However, if clutter intrudes into the track gate, it will give rise to a significant difference video sum. Thus, the difference video is accumulated over the track gate and this clutter detection information is sent to the microcomputer function for use in various correlation tracking control algorithms and in overall tracking processor mode and track state control.

Scene-averaged video from the correlation recursive reference and the correlation difference video are intrinsic to the matched filter correlation algorithm. When these video output byproducts are combined with a centroid processing function, the result is the means to implement a number of unique and potentially useful tracking functions or modes via microcomputer firmware. Thus, the means to route the recursive reference video and the absolute value of the difference video to the centroid processor via a video bus has been incorporated into the tracking processor design. The correlation recursive reference video and the basic difference video outputs are also available via the video bus, as instrumentation video.

### 5. Microcomputer Processing Function

The microcomputer and timing and control function provides a capable microcomputer and proven firmware for executing the indicated tracking error computations, specific processor related functional control algorithms, overall dual-mode processor control, and automatic built-in test.

In addition, input/output provisions for communication with a mission computer, servo electronics, and/or operator's console are supported. Hardwired circuitry is also provided to generate automatic built-in-test video and timing and control signals required by the other processor functional blocks.

An Intel 80186 highly integrated 16-bit microcomputer supported with 16K bytes of RAM and 128K bytes of PROM is utilized to implement the microcomputer function. The integrated feature set for the 80186 includes two independent, high-speed direct memory access channels, programmable interrupt controller, three programmable 16-bit timers and programmable memory, and peripheral chip select logic.

The various control algorithms executed in the microcomputer firmware provide:

- 1) Gain and offset control commands for the video preprocessor AGC function
- 2) Video peak and valley detector spatial gating commands for the video preprocessor
- 3) Target contrast and video threshold commands for the centroid processor
- 4) Track and border gate size and position commands for the centroid processor
- 5) Track status indication for the centroid processor
- 6) Recursive reference update rate commands for the correlation processor
- 7) Track and gradient gate size and position commands for the correlation processor
- 8) Track status indication for the correlation processor
- 9) Track loop servo gain and compensation terms
- 10) Track state and/or mode control for the individual error processor and overall processor
- 11) Automatic built-in-test (BIT) control and fault-isolation-test (FIT) for the overall processor.

External interfaces provided by the microcomputer functions are analog track errors or track rate commands, a serial input/output port, parallel input/output ports, analog input/output ports, and the instrumentation video output.

## Appendix C. Image Auto-Tracker Algorithms

### 1.0 Introduction

The Hughes dual mode tracker (DMT) incorporates both centroid and correlation image tracker algorithms. Generally, centroid tracking is used for well defined extended or point targets which can be thresholded and gated, and correlation tracking is required for complex or time-varying extended targets in a cluttered background. Considerations for centroid processing include:

- Spatial gating is usually utilized to exclude background clutter and minimize video noise induced jitter.
- The threshold must be selected such that the target of interest is isolated from the remaining background clutter, otherwise the indicated centroid position is meaningless.
- The track gate must completely enclose the thresholded target, otherwise the indicated centroid position is ambiguous.
- If ultra low jitter performance is not required and these thresholding and gate sizing requirements can be met, centroid processing is the technique of choice.
- Track point is geometrically related to thresholded video image.

Properties of the correlation tracker include:

- Can be implemented as a matched filter process thereby minimizing the angular tracking jitter.
- Insensitive to video threshold settings and to such image fluctuations as glints and contrast centroid shifts.
- Provides the means to track specific portions of extended targets.
- Track point may be ambiguous. That is, it is determined by the location of the reference image when tracking is initiated. After target aspect angle changes, it may change as a function of the update history for the recursive reference.

### 2.0 Correlation Track

In an ideal correlation processor, the cross-correlation function for an incoming video image and a known, stored reference image are generated. The correlation track error is then the reference image angular shift that produces the largest value for the cross-correlation function. Expressed mathematically (in one dimension) the cross-correlation function is:

$$C(\epsilon') = \int_{-\infty}^{\infty} M(\epsilon - \epsilon') S(\epsilon) d\epsilon$$

where

$C(\epsilon')$  is the cross-correlation function

$M(\epsilon - \epsilon')$  is the intensity distribution of the stored reference image  
as a function of angular position ( $\epsilon$ )

$S(\epsilon)$  is the intensity distribution of the incoming image

$\epsilon'$  is the angular displacement between the incoming and reference images

The desired tracking error is the reference image displacement that yields the peak value for the cross-correlation function. So, the tracking error can be determined by differentiating  $C(\epsilon')$  with respect to the reference angular shift ( $\epsilon'$ ). The zero crossing of this new function yields the reference image shift (desired track error) that yields the peak value of the cross-correlation function,  $C(\epsilon')$ .

The derivative of the cross-correlation function is expressed in terms of the derivative of the reference image (M) and the incoming video image (S).

$$\left[ \frac{\partial}{\partial \epsilon'} C(o) \right] = \int_{-\infty}^{\infty} \frac{\partial}{\partial \epsilon'} M(\epsilon) \cdot S(\epsilon) d\epsilon$$

and,

$$\Delta \epsilon = \frac{\left[ \frac{\partial}{\partial \epsilon'} C(o) \right]}{\text{SLOPE}}$$

where

$$\text{SLOPE} = \int_{-\infty}^{\infty} \left[ \frac{\partial}{\partial \epsilon'} M(\epsilon) \right]^2 d\epsilon$$

Since the error processing gate area for actual imaging trackers is limited, and the background levels may not be uniform, the correlation track error algorithm must be modified. This modification consists of using the difference between the incoming video image and the reference image (difference video) rather than using the incoming video image alone. The resulting derivative of the cross correlation function is:

$$\left[ \frac{\partial}{\partial \epsilon'} C'(o) \right] = \int_a^b \frac{\partial}{\partial \epsilon'} M(\epsilon) \cdot [S(\epsilon) - M(\epsilon)] d\epsilon$$

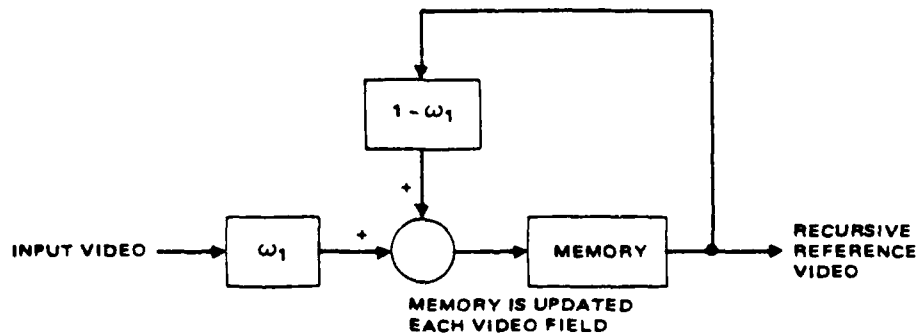
and the slope is:

$$\text{SLOPE} = \int_a^b \left[ \frac{\partial}{\partial \epsilon'} M(\epsilon) \right]^2 d\epsilon$$

where a and b are the track gate boundaries.

### 2.1 Recursive Reference

A recursive reference technique is used to establish the reference image. This technique is illustrated below.

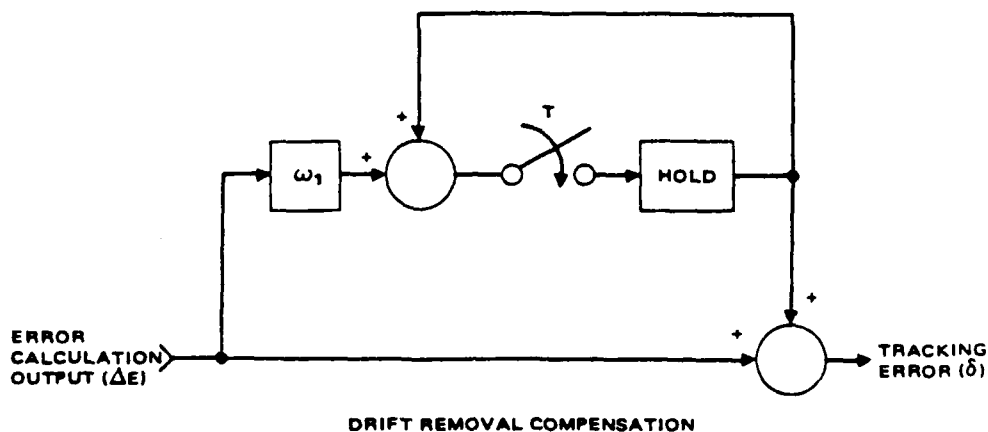


The intensity value for each pixel in the reference image memory is determined by the old intensity value in memory and the intensity value for the corresponding pixel of the incoming video image. The old memory pixel intensity is multiplied by  $(1 - W_1)$  and added to the incoming video image pixel intensity value multiplied by  $W_1$  where  $W_1$  is a number less than or equal to one. If  $W_1 = 1$ ,

the reference image is the incoming video image for the previous frame. If  $W_1 = 0$ , the reference scene remains unchanged. For a  $W_1$  between 0 and 1, the "lifetime" of a given reference image is  $1/W_1$  video frames.

## 2.2 Drift Removal Compensation

Since the recursive reference technique allows the reference image to adapt to the incoming video image as a function of  $W_1$ , it is necessary to keep track of the effective reference image motion. This operation is performed by the drift removal compensation processing illustrated below.



The error signal ( $\Delta\epsilon$ ) is multiplied by  $W_1$ , and the  $W_1 \cdot \Delta\epsilon$  products are accumulated at the video field rate. Then the total correlation track error is the sum of  $\Delta\epsilon$  and the accumulated  $W_1$  weighted errors. Thus, although the track error at the input to the drift remover ( $\Delta\epsilon$ ) is normally maintained at a value less than one pixel, the total output tracking error can be many pixels in magnitude.

## 2.3 Correlation Algorithm

The complete correlation processor is shown in Figure C-1. The recursive reference image is generated by multiplying the values of input video intensity by  $W_1$  and then adding this product to the value of the reference image intensity for the corresponding pixel multiplied by  $(1-W_1)$ . The weighting functions for the azimuth and elevation axes ( $W_d$  and  $W_e$ ) are derived by taking the difference in the values of the reference image intensity for the two pixels adjacent to the pixel of interest and dividing by two to calculate the slope of the reference image intensity. The products of the weighting functions and the difference video are accumulated over the gate area (integrated) to produce the derivative of the cross-correlation function in each axis ( $E_d$  and  $E_e$ ). Similarly the squares of the weighting functions ( $W_d$  and  $W_e$ ) are accumulated over the gate area (integrated) to produce the normalization factors ( $C_d$  and  $C_e$ ). The cross-products of  $W_e$  and  $W_d$  ( $W_e \cdot W_d$ ) are also accumulated to produce a cross-coupling factor ( $C_{ed}$ ). This factor is required to eliminate cross-coupling errors when an extended target is skewed relative to the field of view. Computations in the upper portion of Figure C-1 are performed at the 5.46 MHz pixel rate. Computations in the lower portion of the figure are performed at the 60 Hz video field rate.

## 2.4 Adaptive Reference Weighting Factor ( $W_1$ )

The effective angular misalignment between the incoming video image and the reference image should be maintained at values less than one pixel. To accomplish this, the error terms are used to control the recursive reference  $W_1$  value. As the error approaches one pixel, the  $W_1$  value is increased to allow the reference image to adapt more rapidly. The adaptive reference image weighting factor algorithm is shown in Figure C-2. The drift removal input errors for both axes



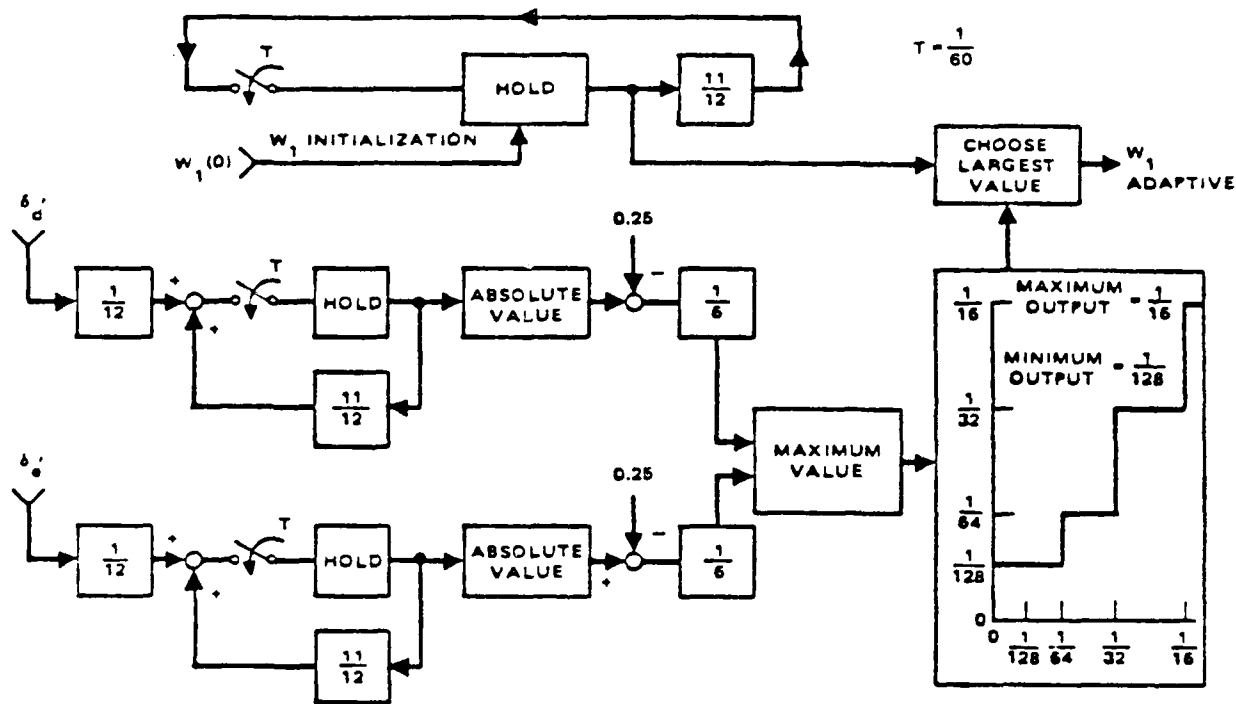
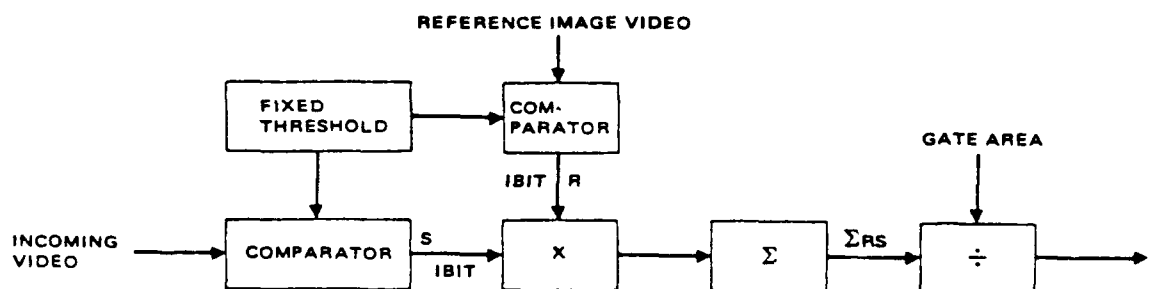


Figure C-2. Adaptive Reference Image Weighting Factor Algorithm

( $\delta d'$  and  $\delta \theta'$ ) are scaled and filtered in a digital implementation equivalent to a first-order lag ( $1/\tau s + 1$ ) with a time constant ( $\tau$ ) of 0.2 second. If the absolute value of either filtered result exceeds 0.34 pixel ( $0.25 + 1/64 + 1/6$ ), a  $W_1$  value greater than  $1/128$  is selected. The maximum value produced by this algorithm is limited to  $1/16$ . The  $W_1$  value selected before the adaptive algorithm mode engagement is read into a  $W_1$  initialization filter. The output of this filter decays exponentially to zero with a time delay of 0.2 second.

## 2.5 Reference Reload and Correlation Track Quality

The reference reload and correlation track quality algorithm is shown below.



The incoming scene video and the reference image videos are compared to a fixed threshold to produce one-bit scene (S) and reference (R) videos. The product (coincidence values) of R and S are accumulated (summed) to produce  $\Sigma RS$ , which is then divided by the track gate area to produce a cross-correlation coefficient, P. If  $P < 0.25$ , a new reference is loaded and the  $W_1$  algorithm is re-initialized. P is also used to estimate track quality. Track quality is used in the autotrack mode to determine which track mode (correlation, centroid, coast) is selected. Table C-1 defines the track quality levels as a function of P.

TABLE C-1. CORRELATION TRACK QUALITY LEVELS

Condition	Track Quality
$0.7 \leq P$	Excellent
$0.5 \leq P < 0.7$	Good
$0.25 \leq P < 0.5$	Impending loss of track
$P < 0.25$	Breaklock. Reload recursive reference and re-initiate the $W_1$ control for adaptive update mode

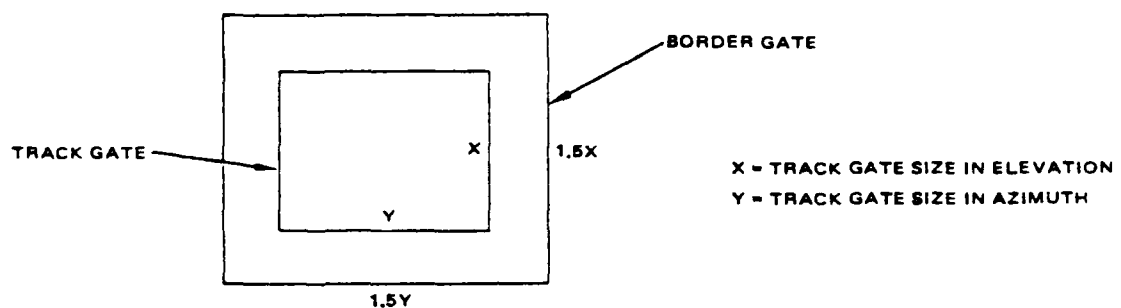
## 3.0 Centroid Track

The centroid track error algorithm is a 1-bit (silhouette centroid) configuration. The incoming analog video image is converted to a 6-bit digital video image in an A/D converter. This 6-bit video is converted to 1-bit video by setting all pixels above a specified threshold equal to unity and all pixels below the threshold equal to zero. The centroid error is generated by weighting each pixel proportional to its distance (azimuth and elevation) from the center of the tracking gate and accumulating (integrating) the weighting factors over the gate area. The result is divided by the image area (the accumulation of all unity-valued pixels) to produce a normalized silhouette-centroid error.

The centroid track error processor, showing the azimuth and elevation functions and associated computational word bit-sizing, is shown in Figure C-3. The azimuth and elevation weighting functions are accumulated over the track gate area at the 5.46 MHz pixel rate to produce the error factors  $E_d$  and  $E_e$ . These are divided by the image area normalization factor ( $I_o$ ) and scaled to produce the azimuth and elevation centroid track errors ( $\delta d$  and  $\delta e$ ).

### 3.1 Centroid Threshold

The centroid threshold algorithm is a dual-gate histogram analyzer. The geometry of the two gates is illustrated below.



Two histograms are generated, one for the track gate, and one for the border gate. The track gate histogram is an array of 32 digital words defining the number of pixels at each of 32 intensity levels within the track gate. The border gate histogram is an array of 32 digital words defining the number of pixels at each of 32 intensity levels within the border gate. Each histogram is smoothed (filtered) using the relationship:

$$H(k) = a H(k) + (1-a) H(k) Z^{-1}$$

where

- $H(k)$  = smoothed histogram array
- $H(k)$  = raw video data histogram array
- $H(k)Z^{-1}$  = last value (previous frame period) of  $H(k)$
- $a$  =  $0 < \text{number} < 1$  defining the filter time constant

Both smoothed histograms (track and border gate) are integrated over the intensity values, starting at the maximum intensity value. The background threshold ( $V_B$ ) is computed as the intensity level at which 5 percent of the pixels in the border gate are above the  $V_B$  intensity. Three video thresholds ( $V_{TL}$ ,  $V_{TI}$ , and  $V_T$ ) are computed as the intensity levels at which 10 percent, 15 percent, and 25 percent of the pixels in the track gate are above the respective intensity levels. Table C-2 defines the centroid track quality levels as a function of  $V_B$ ,  $V_{TL}$ ,  $V_{TI}$  and  $V_T$ . Track quality is used in the autotrack mode to determine which track mode (correlation, centroid, coast) is selected.

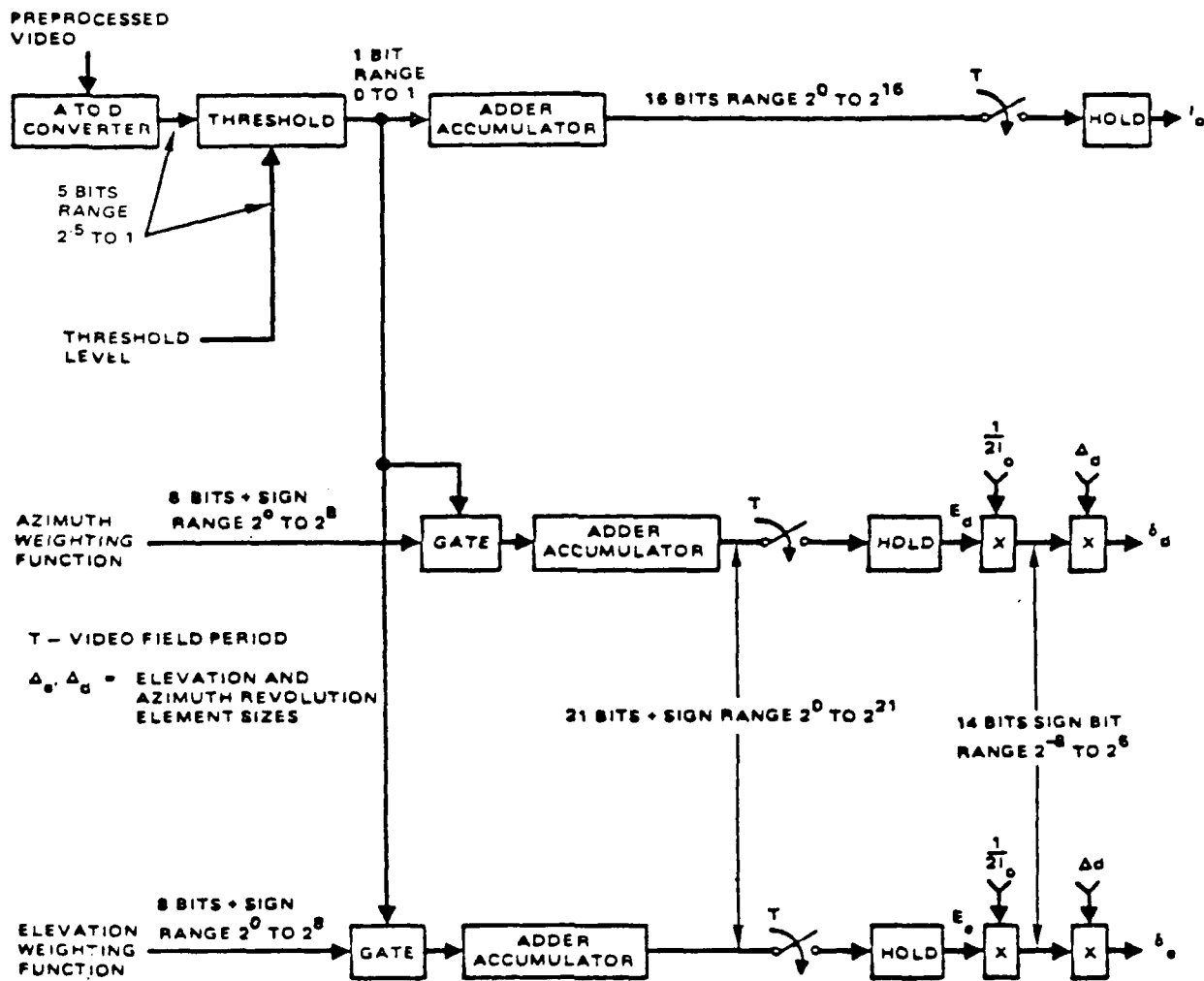


Figure C-3. Centroid Track Error Processor

TABLE C-2. CENTROID THRESHOLD AND TRACK QUALITY LEVELS

<u>Condition</u>	<u>Threshold</u>	<u>Track Quality</u>
$V_T \geq V_B$	$V_T$	Excellent
$V_{TI} \geq V_B > V_T$	$V_B$	Good
$V_{TL} \geq V_B > V_{TI}$	$V_B$	Impending loss of track
$V_B > V_{TL}$	$V_{TL}$	Breaklock

#### 4.0 Track Mode Control

The standard procedure is for the operator to manually track the target to the center of the reticle. He then switches to the autotrack mode and continues to manually track the target until the autotracker locks on.

Centroid tracking acquisition begins immediately when the autotrack mode is selected. Centroid tracking should begin after three video frames are processed (0.1 second). Initial offsets will be reduced to 1 percent in 0.4 second. Centroid tracking continues until the centroid breaklock criterion listed in Table C-2 are satisfied or until the autotrack mode is deselected. The centroid tracker attempts to reacquire automatically after breaklock when in autotrack mode.

Correlation tracking acquisition begins 0.5 second (15 frames) after the autotrack mode is selected. Correlation tracking should begin after two video frames are reprocessed. Correlation tracking continues until correlation breaklock criterion listed in Table C-1 are satisfied or until the autotrack mode is deselected. The correlation tracker attempts to reacquire automatically when in autotrack mode by reloading the reference every 0.5 second if centroid tracking or every 10 seconds if not centroid tracking.

Both centroid and correlation tracking error data are computed whenever breaklock does not exist in the respective mode. Table C-3 lists the logic used in selecting the track mode used in autotracking. The autotracker switches from one mode to another after 6 of 8 successive video frames indicate a mode change should be made. The autotracker switches into or out of coast mode after 3 of 4 successive video frames indicate a mode change should be made. When the source of the video is changed, or FOV is changed, centroid tracking is re-initiated as soon as the new data is available and correlation tracking is re-initiated 7 frames later.

The tracker enters the coast mode when both the centroid and correlation track algorithms indicate a breaklock quality state. The output line-of-sight rate is held constant at the coast mode engage condition while in the coast mode. The tracker enters the position hold mode after 10 seconds of coast mode. The output line-of-sight rate is set to zero during the position hold mode.

TABLE C-3. TRACK MODE SELECT LOGIC

CONDITIONS	QUALITY*		TRACK MODE	REMARKS
	CENTROID	CORRELATION		
$0.7 \leq P$ $V_B \leq V_T$ $P < 0.7$	ANY	EXCELLENT	CORRELATION	RELOAD CORRELATION MAP EVERY 0.5 SECOND AS LONG AS $V_B < V_T$
$V_T < V_B$ $0.5 \leq P < 0.7$	EXCELLENT	GOOD, ITL OR B.L.	CENTROID	
$V_T < V_B$ $0.5 \leq P < 0.7$	GOOD, ITL OR B.L.	GOOD	CORRELATION	RELOAD CORRELATION MAP EVERY 0.5 SECOND
$V_T < V_B < V_{TI}$ $P < 0.5$	GOOD	ITL OR B.L.	CENTROID	
$V_{TI} \leq V_B$ $0.25 \leq P < 0.5$	ITL OR B.L.	ITL	CORRELATION	INDICATE IMPENDING TRACK LOSS
$V_{TI} \leq V_B < V_{TL}$ $P < 0.25$	ITL	B.L.	CENTROID	RELOAD CORRELATION MAP EVERY 0.5 SECOND. INDICATE IMPENDING TRACK LOSS.
$V_{TL} \leq V_B$ $P < 0.25$	B.L.	B.L.	COAST MODE	RE-INITIALIZE MAP AFTER 10 SECONDS OF COAST. INDICATE COAST MODE.
$0.25 < P$ COAST MODE		ITL, GOOD, EXCELLENT	CORRELATION (POSITION HOLD)	TRACKER MAY BE LOCKED ON A FIXED SCENE EQUIVALENT TO POSITION HOLD.

\*IMPENDING TRACK LOSS (ITL), BREAK LOCK (B.L.)